

# CRISPRi-based programmable logic inverter cascade for antibiotic-free selection and maintenance of multiple plasmids

Seong Keun Kim<sup>1,2,†</sup>, Haseong Kim<sup>1,2,†</sup>, Seung Gyun Woo<sup>1,2</sup>, Tae Hyun Kim<sup>1,2</sup>, Eugene Rha<sup>1</sup>, Kil Koang Kwon<sup>1</sup>, Hyewon Lee<sup>1</sup>, Seung-Goo Lee<sup>1,2,\*</sup> and Dae-Hee Lee<sup>1,2,3,\*</sup>

<sup>1</sup>Synthetic Biology Research Center, Korea Research Institute of Bioscience and Biotechnology (KRIBB), Daejeon 34141, Republic of Korea, <sup>2</sup>Department of Biosystems and Bioengineering, KRIBB School of Biotechnology, University of Science and Technology, Daejeon 34143, Republic of Korea and <sup>3</sup>Department of Integrative Biotechnology, College of Biotechnology and Bioengineering, Sungkyunkwan University, Suwon-si, Gyeonggi-do 16419, Republic of Korea

Received June 02, 2022; Revised October 27, 2022; Editorial Decision October 27, 2022; Accepted November 03, 2022

## ABSTRACT

Antibiotics have been widely used for plasmid-mediated cell engineering. However, continued use of antibiotics increases the metabolic burden, horizontal gene transfer risks, and biomanufacturing costs. There are limited approaches to maintaining multiple plasmids without antibiotics. Herein, we developed an inverter cascade using CRISPRi by building a plasmid containing a single guide RNA (sgRNA) landing pad (pSLiP); this inhibited host cell growth by repressing an essential cellular gene. Anti-sgRNAs on separate plasmids restored cell growth by blocking the expression of growth-inhibitory sgRNAs in pSLiP. We maintained three plasmids in *Escherichia coli* with a single antibiotic selective marker. To completely avoid antibiotic use and maintain the CRISPRi-based logic inverter cascade, we created a novel D-glutamate auxotrophic *E. coli*. This enabled the stable maintenance of the plasmid without antibiotics, enhanced the production of the terpenoid, (–)- $\alpha$ -bisabolol, and generation of an antibiotic-resistance gene-free plasmid. CRISPRi is therefore widely applicable in genetic circuits and may allow for antibiotic-free biomanufacturing.

## INTRODUCTION

Recent advances in bioengineering have yielded an eclectic group of genetic circuits to program new biological functions, dynamics and logic control in living cells (1–5). The ability to build various genetic circuits in living cells could

allow engineers to create novel decision-making systems for various applications, including disease diagnostics and treatments based on sensed information and synthetic regulations for the bioproduction of natural products or new classes of chemicals (4,6–9). A fundamental challenge in building complex genetic circuits that execute user-defined functions has been the availability of a large repertoire of transcriptional regulators (TRs) (10–12). TRs should operate with other functional bio-parts in genetic circuits with minimal crosstalk. This can be achieved by building genetic circuits using modular orthogonal TRs (13–15). As most genetic circuits have adopted TRs, the ability to build user-defined genetic circuits has been constrained by the unavailability of synthetic TRs that can be orthogonal to the host and regulate any sequence of interest in DNA at the desired level of expression (16,17).

Recently, the nuclease-deactivated Cas9 (dCas9) effector protein has been used in CRISPR interference (CRISPRi) (18,19) and CRISPR activation (CRISPRa) (19,20) as a programmable and orthogonal synthetic TR (21–24). In these systems, dCas9 loses its endonuclease activity while maintaining its ability to form complexes with single guide RNAs (sgRNAs), ultimately leading to target DNA binding. In CRISPRi, the dCas9/sgRNA ribonucleoprotein complex is recruited to the promoter or coding regions of a gene of interest to interfere with the recruitment or progression of RNA polymerase (RNAP). This results in the transcriptional inhibition of the gene of interest (18). By using programmable dCas9-mediated transcriptional repression, novel logic circuits have been constructed to control complex cellular behaviors (25–28). For example, the CRISPR-Cas9 AND gate was built to function in bladder cancer cells using two input promoters (25). The AND gate activates an output that produces a cellular phenotype only when both

\*To whom correspondence should be addressed. Tel: +82 42 860 4373; Fax: +82 42 860 4489; Email: sglee@kribb.re.kr

Correspondence may also be addressed to Dae-Hee Lee. Tel: +82 42 879 8225; Fax: +82 42 860 4489; Email: dhlee@kribb.re.kr

†The authors wish it to be known that, in their opinion, the first two authors should be regarded as Joint First Authors.

promoters can drive gene expression in the tested cell lines. By using this CRISPR-Cas9 AND gate circuit, functional genes promoting cell death are expressed only in bladder cancer cells to induce apoptosis and decrease cell motility (25,29). Besides AND gate (30), the modular NOT and NOR gates have been created with the CRISPR-dCas9 system to control cellular physiologies, such as sugar utilization, chemotaxis, and phage susceptibility (31).

Genetic circuits, including toggle switches, oscillators, light-sensitive networks, and logic gates, are often created using plasmids (32–34) that are easier to design, build, test, and tune compared to chromosomally integrated DNA. As genetic circuits become increasingly complex, multiple plasmids are frequently required to house the bio-parts of the circuits. However, the use of plasmids limits the ease with which they are placed into microbial hosts because selective markers must be encoded for each plasmid to maintain them in the host. These unique selective markers are often antibiotic-resistance genes. Antibiotics and antibiotic-resistance genes are commonly used to select and maintain recombinant plasmids in hosts. However, their continued use is a major issue in the era of the bio-based economy (35–37) because of the following reasons: (i) the risk of horizontal transfer of antibiotic-resistance genes can spur the emergence of multidrug-resistant microorganisms (38); (ii) the use of antibiotics for biotechnological applications increases the production cost of value-added bioproducts in large-scale fermentation (39) and (iii) the constitutive expression of antibiotic-resistance genes imposes a metabolic burden on hosts, which results in decreased metabolic productivity (40).

To produce bioproducts using microbes, metabolic pathways can be chromosomally integrated to eliminate the use of antibiotics for plasmid maintenance along with stable expression and reduced cell-to-cell variability. However, chromosomal integration often requires multiple integration of target metabolic pathways to achieve sufficient product titer (41,42). Furthermore, these genome engineering processes are laborious, which limits rapid prototyping of the different metabolic constructs and host strains. Therefore, the development of plasmid-based antibiotic-free production systems that allow flexibility to tweak and tune the genetic constructs to improve the titer and productivity of target biochemicals is required.

Currently, there are several methods for the antibiotic-free selection and maintenance of single plasmid in microbial cells (35,37,43–45). These include auxotrophy complementation, which is based on auxotrophic strains for cellular anabolism (for cell walls, amino acids, and DNA precursors). Auxotrophy complementation is created by mutating or knocking out corresponding chromosomal genes, which can be complemented with their plasmid-borne equivalents. However, these methods to create auxotrophic strains are laborious and usually require defined media for plasmid maintenance that are not used for bioproduction (37). Another method is post-segregational killing, which relies on the balance between toxins and antitoxins that are expressed in chromosomes and plasmids, respectively. If a cell loses a plasmid encoding an antitoxin, the toxin will kill the cell. An additional method includes operator-repressor titrations,

which use plasmids with the *lac* operator to derepress essential chromosomal genes (44). The loss of plasmids results in halted titrations of the repressor and causes cell death. However, these are not suitable for the stable selection and maintenance of multiple plasmids. A previous study reported the stable maintenance of three different plasmids in *Escherichia coli* using a single antibiotic selective marker (46). In this system, the kanamycin-resistance gene was split into two fragments encoded on two plasmids that were transcribed by T7 RNAP in another plasmid. However, this method still used antibiotics and antibiotic-resistance genes, and the large sizes of the T7 RNAP gene limited their applicability. In addition, this method was incompatible with a protein expression system based on the use of T7 RNAP.

Here, we developed a novel antibiotic-free system to select and maintain multiple plasmids using the CRISPR-dCas9 inverter (NOT gate) cascade. We first built a modular NOT logic gate using a CRISPR-dCas9 system that inhibited cell growth by repressing the transcription of essential genes. We then created a NOT gate cascade by adding a secondary NOT gate to repress the primary NOT gate that repressed the transcription of essential genes, which restored cell growth. Next, we generated a novel D-glutamate (D-Glu) auxotrophic *E. coli* strain that can be used for the CRISPR-dCas9 inverter cascade to maintain multiple plasmids without the use of antibiotics and antibiotic-resistance genes. Finally, we explored the applicability of the developed antibiotic-free system by producing a molecule of interest in engineered *E. coli* without the use of antibiotics.

## MATERIALS AND METHODS

### Bacterial strains and reagents

The *E. coli* DH5 $\alpha$  bacterial strains were used for cloning and plasmid maintenance. The *E. coli* strains DH5 $\alpha$  and WM335 were used for (–)- $\alpha$ -bisabolol production. Lysogeny broth (LB) medium (containing 10 g/l tryptone, 5 g/l yeast extract, and 10 g/l sodium chloride) was used for all experiments except those with specific indications. MOPS EZ Rich Defined (EZ) medium (Teknova, Hollister, CA, USA) was used per the manufacturer's protocol without ACGU solution. To produce (–)- $\alpha$ -bisabolol, terrific broth containing glycerol (TBG) medium (containing 12 g/l enzymatic casein digest, 24 g/l yeast extract, 9.4 g/l K<sub>2</sub>HPO<sub>4</sub>, 2.2 g/l KH<sub>2</sub>PO<sub>4</sub>, and 3.5% (w/v) glycerol) was used. SOC medium (containing 20 g/l tryptone, 5 g/l yeast extract, 0.5 g/l sodium chloride, 2.4 g/l magnesium sulfate, 186 mg/l potassium chloride and 4 g/l glucose) was used as a recovery medium after the transformations. L-Rhamnose and antibiotics were purchased from Sigma-Aldrich (St. Louis, MO, USA). Ampicillin was used at a concentration of 100  $\mu$ g/ml; chloramphenicol at 34  $\mu$ g/ml; and kanamycin at 25  $\mu$ g/ml, unless specified otherwise. For the polymerase chain reaction, high fidelity KOD-Plus-Neo polymerase (Toyobo, Osaka, Japan) was used with the standard protocol. All restriction and modification enzymes were purchased from New England BioLabs (NEB, Ipswich, MA, USA).

## Plasmid construction

The oligonucleotides and plasmids used in this study are listed in Supplementary Tables 1 and 2, respectively. Plasmid sequences are provided in the Supplementary Information. All the binding sites of the sgRNAs used for CRISPRi are listed in Supplementary Table 3. The CRISPRi plasmid construction was based on a previously reported method (47). In brief, a CRI-F and CRI-R primer pair was used for PCR amplification from a pSECRi plasmid to change the sgRNA region. Primer pairs with PAM-F and PAM-R were used to introduce a PAM sequence to the J23119 promoter, resulting in a pSLiP plasmid. After amplification, the appropriate band was extracted from the gel using the Wizard® SV Gel and PCR Clean-Up System (Promega, Madison, WI, USA). After gel purification, the PCR fragment was treated using DpnI and ligated using T4 DNA ligase and T4 polynucleotide kinase.

For the sgRNA assembly, pSLiP(sgRNA1) was treated with XmaI and NcoI, and the fragment containing a sgRNA1 expression cassette was gel extracted. pSLiP(sgRNA2) was treated with AgeI and NcoI, and the fragment containing a sgRNA2 expression cassette was gel extracted. The two extracted fragments were ligated, resulting in a pSLiP(sgRNA1 + sgRNA2) plasmid.

For the *racE* expression in pSLiP, we inserted the BioBrick\_J23100 promoter in front of *racE* in a pGESS-DAAT plasmid. To achieve this, we amplified the entire region of the pGESS-DAAT plasmid using pDAAT-F and pDAAT-R primers which contained the BioBrick\_J23100 promoter sequence. The amplified fragment was then purified and ligated using T4 DNA ligase/T4 polynucleotide kinase, resulting in a pGESS-J23100-RacE plasmid. From this plasmid, we amplified the J23114-RacE cassette using RacE-F and RacE-R primers which contained BioBrick\_J23114 promoter sequences instead of the BioBrick\_J23100 promoter. These were assembled into a pSLiP plasmid which was digested with PacI using the Gibson Assembly Method (NEB) as per the manufacturer's instructions.

The pT-GFP plasmid was constructed as follows. The vector region was amplified using pTSN-sf-VF and pTSN-sf-VR primers and a pT-BBS plasmid template. The GFP region was amplified using pTSN-sf-IF and pTSN-sf-IR primers and a pK7 sfGFP plasmid. The two fragments were then assembled using the Gibson Assembly method as per the manufacturer's instructions.

For the construction of the pA-RFP plasmid, the vector region was amplified using pACBB-ch-VF and pACBB-ch-VR and a pACBB-eGFP plasmid template. The mCherry region was amplified using pACBB-ch-IF and pACBB-ch-IR primers and a pCherΔlacI plasmid. The two fragments were then assembled using the Gibson Assembly method.

To repress the expression of sgRNA in the pSLiP-A2 plasmid, we changed the sgRNA region of pgRNA-bacteria. To achieve this, we amplified the entire region of pgRNA-bacteria using a sgKan2AGG-F and sgKan2AGG-R primer pair. The correct band size was purified and ligated using T4 DNA ligase and T4 polynucleotide kinase, resulting in the pgRNA-rA2 plasmid.

For the sgRNA-tagging in the pT-GFP plasmid, we constructed a CRISPRi plasmid that could bind the sgRNA

of a pSLiP plasmid using rCRI-F and rCRI-R primers from the pSECRi plasmid as per the aforementioned protocol. We then amplified the sgRNA cassette region using sgRNA(GFP)-F and sgRNA(GFP)-R primers and assembled them into a pT-GFP plasmid which was digested with XbaI using the Gibson Assembly method.

For the sgRNA-tagging in the pA-RFP plasmid, we constructed a CRISPRi plasmid to bind the sgRNA on the pSLiP plasmid using rCRI-F and rCRI-R primers from the pSECRi plasmid as per the aforementioned protocol. We then amplified the sgRNA expression cassette region using sgRNA(RFP)-F and sgRNA(RFP)-R primers. The vector region was amplified by using mCherry-VF and mCherry-VR using a pA-RFP template. The two fragments were assembled using the Gibson Assembly method.

For the sgRNA-tagging into pTM-BBS, we amplified the sgRNA expression cassette region using sgRNA(BIS)-F and sgRNA(BIS)-R primers from the pSECRi plasmid containing the sgRNA cassette. We then assembled the amplified fragment into the pTM-BBS digested with SbfI.

For inserting GFP and sgRNA into pTM-BBS and pTSN-Bisa-Sa, we amplified the GFP and sgRNA expression cassette region using GFPsgRNA(BIS)-F and GFPsgRNA(BIS)-R primers from the pT-GFP-rG2 plasmid. The amplified fragment was then assembled into pTM-BBS or pTSN-Bisa-Sa, both of which were digested with SbfI.

For inserting RacE and GFP into pTSN-Bisa-Sa and pTSN-Bisa-Mm, we amplified the RacE and GFP using DG-F and DG-R primers from the pGESS-DAAT plasmid. The amplified fragment was then assembled into pTSN-Bisa-Sa or pTSN-Bisa-Mm, both of which were digested with SbfI.

For the pKI-mGltS-Cm plasmid construction, we amplified the backbone region containing the chloramphenicol resistance gene from the pKD3/I-SceI plasmid using KI-VF and KI-VR primer pairs. We also amplified a mutated *gltS* from WM335 genomic DNA using KI-IF and KI-IR primer pairs. The two amplified fragments were then assembled using the Gibson Assembly method.

## Cell growth inhibition assay

*E. coli* DH5α cells were transformed with a pSLiP plasmid and selected on an LB plate containing 25 μg/ml kanamycin. A single colony was inoculated into LB medium supplemented with 25 μg/ml kanamycin and 1 mM L-rhamnose. The cells were incubated overnight at 30°C with shaking at 200 rpm. Pre-cultures were inoculated (0.1% v/v) into an LB medium containing various kanamycin concentrations and 1 mM L-rhamnose. They were then incubated for 11 h at 30°C with shaking at 200 rpm. The optical density of cell growth was measured using a Victor X multi-label plate reader (PerkinElmer, Waltham, MA, USA).

For the inverter system using an essential gene, *E. coli* was transformed with a pSLiP plasmid and selected on an LB plate containing 25 μg/ml kanamycin. A single colony was inoculated into LB or EZ medium supplemented with 25 μg/ml kanamycin and 4 mM L-rhamnose. The cells were then incubated overnight at 30°C with shaking at 200 rpm.



The cultured cells were inoculated into LB (0.1% v/v inoculum) or EZ (1% v/v inoculum) medium containing 25 µg/ml kanamycin and 4 mM L-rhamnose. They were then incubated for 11 h at 30°C with shaking at 200 rpm. The optical density of cell growth was measured using a Victor X multi-label plate reader or Infinite 200 PRO microplate reader (Tecan, Männedorf, Switzerland) for the time-course monitoring of cell growth.

### Fluorescence microscopy analysis

*E. coli* DH5α cells with a pSLiP plasmid were co-transformed with a sgRNA-tagged GFP plasmid and mCherry expressing plasmid and recovered using 1 ml of SOC medium. Afterward, 40 µl of transformed cells were inoculated into 5 ml of LB medium supplemented with 200 µg/ml kanamycin and 4 mM L-rhamnose. They were then incubated at 30°C with shaking at 200 rpm. After two more serial cultures, cultured cells were spread on a selection plate (LB plate supplemented with 200 µg/ml kanamycin and 4 mM L-rhamnose). Images of the colonies were obtained using an AZ100M fluorescence multi-zoom microscope (Nikon, Tokyo, Japan) equipped with a GFPHQ filter (455–485 nm excitation, 500–545 nm emission) and TRITC filter (540/25 nm excitation, 605/55 nm emission). For the CRISPRi-based inverter cascade using an essential gene, the same procedure was performed with the only difference being the kanamycin concentration (25 µg/ml instead of 200 µg/ml).

For the single-cell imaging shown in Figure 4F, cultured cells were observed using an Axio Observer microscope (Carl Zeiss, Oberkochen, Germany) under differential interference contrast (DIC) imaging conditions. Fluorescence imaging was also performed with a GFP filter (excitation BP 470/20, beam splitter FT 493, and emission BP 505–530). Image acquisition and region-of-interest analyses were performed using the MetaMorph software (Molecular Devices, Sunnyvale, CA, USA).

### Flow cytometry analysis

*E. coli* DH5α cells were co-transformed with a pSLiP and sgRNA-tagged GFP expressing plasmid and recovered using 1 ml of SOC medium. Afterward, 40 µl of transformed cells were inoculated into 5 ml of LB medium supplemented with 200 µg/ml kanamycin and 1 mM L-rhamnose. The cells were then incubated at 30°C with shaking at 200 rpm. After two more serial cultures on the same medium, a single-cell fluorescence analysis was performed using FACSCalibur (BD Bioscience, Franklin Lakes, NJ, USA) and the FlowJo software (Tree Star, OR, USA).

### (–)-α-Bisabolol production

*E. coli* DH5α strains harboring the pTM-BBS-rA2 and pSLiP-A2 plasmids were individually inoculated onto LB medium supplemented with 100 µg/ml ampicillin, 200 µg/ml kanamycin, and 4 mM L-rhamnose. They were grown at 37°C with shaking at 200 rpm overnight. The cultures were then diluted (1:100) with TBG medium supplemented with 100 µg/ml ampicillin, 200 µg/ml kanamycin,

4 mM L-rhamnose, and 20% (v/v) *n*-dodecane (Sigma-Aldrich) to extract (–)-α-bisabolol from the culture broth. They were then grown at 37°C with shaking at 200 rpm for 2 days. After cultivation, cell growth was measured using a spectrophotometer (Ultrospec 8000, GE Healthcare, Uppsala, Sweden). Single-cell imaging and fluorescence were analyzed using fluorescence microscopy and flow cytometry, respectively. The (–)-α-bisabolol concentration was determined using gas chromatography. For the CRISPRi-based inverter cascade using an essential gene, the same procedure was performed with the only difference being the kanamycin concentration (25 µg/ml instead of 200 µg/ml).

As shown in Figure 5, *E. coli* WM335 strains harboring the pTSNG-Bisa-Sa-rG2 and pSLiP-G2-RacE plasmids were individually inoculated onto LB medium with various combinations of ampicillin and L-rhamnose (0 µg/ml ampicillin and 0 mM L-rhamnose, 0 µg/ml ampicillin and 4 mM L-rhamnose, 100 µg/ml ampicillin and 0 mM L-rhamnose, and 100 µg/ml ampicillin and 4 mM L-rhamnose). They were grown at 30°C with shaking at 200 rpm overnight. The cultures were then diluted (1:100) with TBG medium with the same concentrations of ampicillin and L-rhamnose and 20% (v/v) *n*-dodecane to extract (–)-α-bisabolol from the culture broth. They were then grown at 30°C with shaking at 200 rpm for 2 days. After cultivation, cell growth was measured using a spectrophotometer and single-cell fluorescence was analyzed using flow cytometry. The (–)-α-bisabolol concentration was determined using gas chromatography.

### (–)-α-Bisabolol quantification

The concentrations of (–)-α-bisabolol were determined based on previously described methods (18). In brief, *n*-dodecane was overlaid in the culture medium to extract (–)-α-bisabolol produced from *E. coli*. After cultivation, the *n*-dodecane layer was recovered by centrifugation at 14,500 × *g* for 3 min. The (–)-α-bisabolol amount extracted in the *n*-dodecane layer was determined using a gas chromatography (7890B, Agilent, SC, USA) system equipped with a flame ionization detector (FID) with an HP-5 column (30 m × 0.320 mm × 0.25 µm) and a flow rate of 1 ml/min. The starting temperature of the oven was 60°C for 2 min. This was increased by 5°C/min to 200°C, held at 200°C for 2 min, raised by 50°C/min to 300°C, and held at 300°C for 5 min. The concentrations of (–)-α-bisabolol (Sigma-Aldrich) were used to generate a standard curve.

### Construction of the D-Glu auxotrophic *E. coli* strains

D-Glu auxotrophic *E. coli* was generated using the genome engineering method based on λ Red-mediated homologous recombination (48). A DNA fragment containing the chloramphenicol resistance (*cat*) gene and mutant *gltS* gene was PCR-amplified from the pKI-mGltS-Cm plasmid using gene-specific primers which harbor homologous arms to the *murI* gene. After PCR amplification and agarose gel electrophoresis, the DNA fragment with the correct band size was purified from the gel using Wizard® SV Gel and PCR Clean-Up System (Promega, Madison, WI). The purified DNA fragment was treated with DpnI and purified

using Wizard® SV Gel and PCR Clean-Up System. The DNA fragment containing the *cat* and mutant *gltS* genes was integrated into the *murI* genomic locus of *E. coli* DH5 $\alpha$  via  $\lambda$  Red-mediated homologous recombination. After that, the D-Glu auxotrophic *E. coli* DH5 $\alpha$  candidates were selected on an LB plate supplemented with chloramphenicol (10  $\mu$ g/ml) and D-Glu (50  $\mu$ g/ml). The engineered strains were further verified by colony PCR using strain-specific primers. The *cat* gene was then removed by FLP recombinase encoded from the pCP20 plasmid.

### D-Glutamate auxotrophy in complex media

*E. coli* strains were individually inoculated onto LB medium containing D-Glu (50  $\mu$ g/ml) and grown at 37°C with shaking at 200 rpm overnight. The cells were recovered by centrifugation at 2000  $\times g$  for 20 min and resuspended in LB medium. The resuspended cells were diluted (1:100) with three complex media (LB, TB and 2 $\times$  YT) and cultured at 37°C with shaking at 200 rpm. Cell growth at 600 nm was determined using a spectrophotometer or the Infinite 200 PRO microplate reader for the time-course monitoring of cell growth.

### Statistical analysis

Three to eight replicates were performed independently for each experiment in this study and the data were expressed as mean  $\pm$  SD. Statistical data analysis was carried out with two-tailed *t*-tests (Welch two sample *t*-test). The dataset under the Welch two sample *t*-test was assumed random, independence, normality, and unequal variance.

## RESULTS

### CRISPRi-based double inverter circuits

Microbial cells that lack genetically encoded antibiotic-resistance determinants cannot grow in media containing antibiotics. This is because antibiotics inhibit cell growth by interfering with the synthesis of cell walls (49) and essential proteins (50) (antibiotic-based single inverter). However, cells that carry antibiotic-resistance genes via plasmids can grow in the same media by degrading or modifying antibiotics (51) (antibiotic-based double inverter) (Figure 1A). We employed a synthetic repressor, the CRISPRi system (Figure 1B), to build cascaded logic inverters and mimic the regulation between antibiotics and antibiotic-resistance genes. A single inverter plasmid was created to inhibit cell growth by CRISPRi using a low copy pSEVA221 plasmid and to characterize its performance in an inverter gate (Figure 1C). pSEVA221 contained *aphA* and *trfA* for kanamycin resistance and the replication initiation of the plasmid, respectively. *Streptococcus pyogenes* dCas9 and sgRNA, under the control of an L-rhamnose-inducible *rhaBAD* ( $P_{rhaBAD}$ ) and constitutive Biobrick promoter, respectively, were inserted into pSEVA221 to implement the CRISPRi (pSECRi). Importantly,  $P_{rhaBAD}$ -dependent dCas9 expression did not affect the cellular abnormality in the presence of 4 mM L-rhamnose in contrast to the dCas9 toxicity using the  $P_{tet}$  promoter (Supplementary Figure 1) (52).

The *aphA* gene in the same plasmid was chosen as the target gene of CRISPRi repression to create the CRISPRi-based inverter gate. The *aphA* gene encodes an aminoglycoside 3'-phosphotransferase that inactivates kanamycin by modifying its chemical structure (53). Therefore, cells with repressed *aphA* may be sensitive to kanamycin, including the cells that harbor the plasmid. To repress the expression of *aphA* in pSECRi, two sgRNAs (sgRNA-A1 and sgRNA-A2) targeted non-template DNA strands near the N-terminus of the gene. Cell growth was monitored in the presence of kanamycin ranging from 25 to 500  $\mu$ g/ml while the dCas9 protein was expressed to activate the inverter gate by adding 1 mM L-rhamnose (Figure 1D). The growth of the control *E. coli* cells with empty plasmids was inhibited by up to 35% as the kanamycin concentrations increased up to 500  $\mu$ g/ml. However, the *E. coli* cells harboring the CRISPRi-based inverter plasmid, pSECRi, with sgRNA-A1 or sgRNA-A2 exhibited severe growth inhibition as the kanamycin concentrations increased from 25 to 500  $\mu$ g/ml. In the presence of 200  $\mu$ g/ml kanamycin, the growth of the *E. coli* cells was inhibited by up to 89% for sgRNA-A1 and 93% for sgRNA-A2 (Figure 1D). Although the growth of the cells was further inhibited by CRISPRi-based *aphA* repression at a concentration of 500  $\mu$ g/ml kanamycin (93% for sgRNA-A1 and 96% for sgRNA-A2), the control *E. coli* also showed up to 35% inhibited growth. The sgRNA-A2 was more effective at repressing *aphA* than the sgRNA-A1 in all tested conditions. Therefore, kanamycin at a concentration of 200  $\mu$ g/ml and sgRNA-A2 were used for subsequent experiments for the CRISPRi-based inverter targeting *aphA*. To build cascaded logic inverters using the CRISPRi system, we inserted a protospacer adjacent motif (PAM) between the sgRNA and its promoter ( $P_{J23119}$ ) in the inverter plasmid. This was achieved by changing the DNA sequence of the SpeI restriction enzyme site, at AGG or TGG, which resulted in a pSLiP (plasmid containing a sgRNA landing pad) (Figure 1E). This nucleotide mutation had no effect on the repression of *aphA* by CRISPRi (Figure 1F). The pSLiP possessed two features: (i) it expressed the sgRNA (e.g. sgRNA-A2), which formed a complex with dCas9 to inhibit host cell growth and (ii) it allowed another sgRNA (anti-sgRNA, e.g. sgRNA-rA2) to bind the PAM sequence in the promoter of the growth-inhibitory sgRNA (e.g. sgRNA-A2). This led to the restoration of cell growth by repressing the growth-inhibitory sgRNA (e.g. sgRNA-A2) (Figure 1G). By using pSLiP, we built cascaded logic inverters. We first created a pSLiP-A2 by introducing the sgRNA-A2 into pSLiP and another plasmid expressing the sgRNA-rA2 (pgRNA-rA2). The latter could repress the expression of sgRNA-A2 in pSLiP. We then monitored the growth of *E. coli* cells containing both pSLiP-A2 and pgRNA-rA2. The *E. coli* cells containing both pSLiP-A2 and pgRNA-bacteria (non-targeting sgRNA, single inverter) plasmids exhibited growth defects at various concentrations of kanamycin (25–500  $\mu$ g/ml) (Figure 1H). Conversely, the coexistence of pSLiP-A2 and pgRNA-rA2 restored the growth of the *E. coli* cells at all tested concentrations of kanamycin (Figure 1H). Overall, we successfully built a CRISPRi-based inverter cascade that mimicked the regulation between antibiotics and antibiotic-resistance genes and validated its performance in *E. coli*.

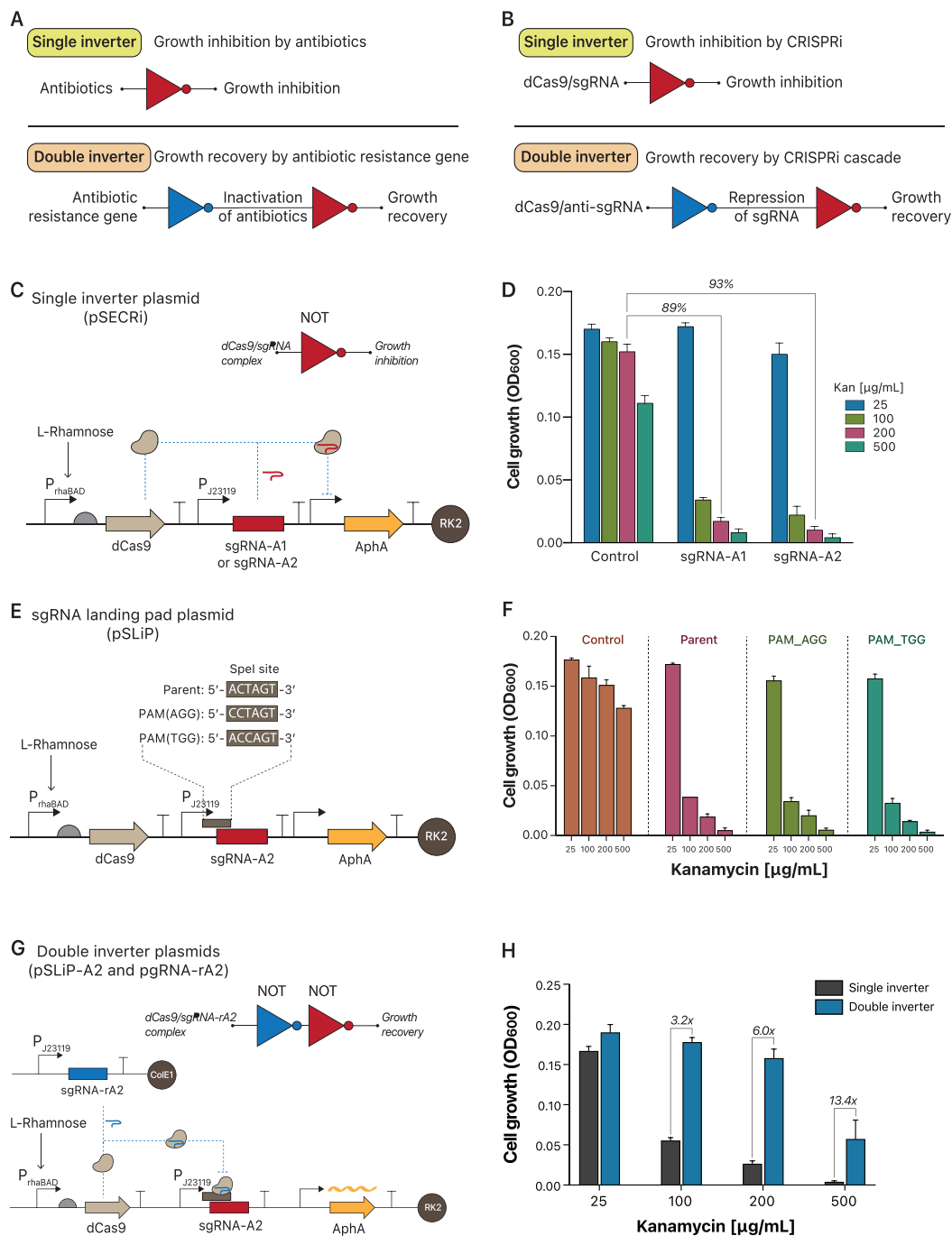


**Figure 1.** Design and construction of the CRISPRi-based inverter cascade. (A) The action of antibiotic-resistance genes against antibiotics can be interpreted as an inverter (NOT gate) cascade in synthetic biology. (B) CRISPRi-based inverter cascades can mimic the relationship between antibiotics and antibiotic-resistance genes. (C) A single inverter plasmid (pSECRi) contained dCas9 under the control of an L-rhamnose-inducible promoter and a sgRNA. In pSECRi, the sgRNA-A1 or sgRNA-A2 targets to repress *aphA*. In the presence of L-rhamnose, *E. coli* cells harboring pSECRi were susceptible to kanamycin given the repression of *aphA* by CRISPRi. (D) Kanamycin susceptibility of *E. coli* cells harboring pSECRi was examined with different concentrations of kanamycin in the presence of L-rhamnose (dCas9 expression). Two independent biological replicates are represented. sgRNA-A1 and sgRNA-A2 are all statistically significant as the *p*-values of the *t*-tests are 0.002 and 0.001, respectively (Source Data File). The control experiment was conducted with *E. coli* cells containing the empty plasmid, pSEVA221. (E) pSLiP was constructed by grafting PAM sequences (AGG or TGG) into an upstream *SpeI* site of the sgRNA in the pSECRi plasmid. (F) The effect of the PAM sequence introduction on *aphA* repression was probed in the LB medium. All the *p*-values of the *t*-test are significant with 0.05 significant level (Source Data File). (G) The CRISPRi-based double inverter system contained two plasmids: pSLiP-A2 and pgRNA-rA2. The pgRNA-rA2 plasmid contained a sgRNA-rA2 that could bind the pSLiP-A2 plasmid and make the sgRNA-A2 of pSLiP-A2 not repress *aphA* in the same plasmid, resulting in *E. coli* cell growth. (H) Growth recovery of *E. coli* cells under the CRISPRi-based double inverter was examined. Two independent biological replicates are represented. The cell growth with both pSLiP-A2 and pgRNA-rA2 are all significantly different from those of single inverter with *p*-values of 0.068, 0.001, 0.013 and 0.096, in kanamycin concentrations of 25, 100, 200 and 500 µg/ml, respectively (Source Data File). The single inverter experiment was conducted with *E. coli* cells containing both pSLiP-A2 and pgRNA-bacteria plasmids (non-targeting sgRNA).



## Selection of multiple plasmids

We examined whether the CRISPRi-based inverter cascade could select a small population of cells transformed with the anti-sgRNA-tagged plasmid encoding  $\beta$ -lactamase from untransformed cells without the use of ampicillin. To accurately and easily measure the individual cells containing the anti-sgRNA-tagged plasmid, a green fluorescent protein (GFP) was expressed in the plasmid expressing sgRNA-rA2 (pT-GFP-rA2). This plasmid was co-transformed with pSLiP-A2 (Figure 2A). The transformed cells were grown for three serial culture transfers with 200  $\mu$ g/ml kanamycin for CRISPRi selection. The green fluorescence at the single-cell level was measured for the distribution of the cell populations containing pT-GFP-rA2 in the culture. In the absence of L-rhamnose and ampicillin, the cells that initially showed approximately 10% fluorescence were not enriched (Figure 2B), as the cascaded inverter gate did not function without the expression of dCas9. In the presence of L-rhamnose, cells containing the anti-sgRNA-tagged plasmid were enriched by 46% at the second transfer. The fluorescence distribution at the third transfer was similar to that of the cells enriched by ampicillin-based selection (Figure 2B). For the plasmid without the anti-sgRNA-tag, the transformed cells were not enriched during the serial transfer regardless of the presence of L-rhamnose (Figure 2B). Genetic circuits using the CRISPR-dCas9 complex enable orthogonal modular gene repression according to the sequence of sgRNAs (21). We used this advantage to select and maintain multiple plasmids in *E. coli* cells through the CRISPRi-based inverter cascade gate. Once we confirmed that the cascaded inverter allowed *E. coli* cells to be enriched by the selection pressure of the anti-sgRNA-tagged single plasmid, we examined the ability of the cascaded inverter gate to enrich cells containing multiple plasmids from minor transformed cells. For this purpose, we constructed pSLiP-A1A2, which simultaneously expressed two sgRNAs (sgRNA-A1 and sgRNA-A2) for the repression of *aphA*. An anti-sgRNA (sgRNA-rA1 or sgRNA-rA2) repressing the expression of sgRNA-A1 or sgRNA-A2 in pSLiP-A1A2, respectively, was cloned to generate a pA-RFP-rA1 or pT-GFP-rA2 expressing mCherry (red fluorescence) or GFP (green fluorescence), respectively (Figure 2C). After the transformation of pA-RFP-rA1 and pT-GFP-rA2 into *E. coli* cells harboring the pSLiP-A1A2, 200  $\mu$ g/ml kanamycin was used as the CRISPRi selection pressure to enrich the transformed cells. After the CRISPRi selection, the majority of the cells showed green and red fluorescence, which indicated that *E. coli*-pSLiP-A1A2 cells containing both pA-RFP-rA1 and pT-GFP-rA2 could grow only in the presence of L-rhamnose because of the derepression of *aphA* (Figure 2D, lower). In the absence of L-rhamnose, most of the cells did not show fluorescence, only some cells showed green or red fluorescence, and very few cells showed yellow fluorescence following the simultaneous expression of GFP and mCherry (Figure 2D, upper). Overall, three plasmids (pSLiP-A1A2, pA-RFP-rA1 and pT-GFP-rA2) were selected in *E. coli* using a single antibiotic (200  $\mu$ g/ml kanamycin) through the CRISPRi-based inverter cascade system.

## Reduction of antibiotic dependency

Following the derepression of *aphA*, the cascaded logic inverter gate required 200  $\mu$ g/ml kanamycin to efficiently select multiple plasmids tagged with anti-sgRNAs. To ease the strong dependency of kanamycin in the CRISPRi-based inverter cascade, we employed a cellular essential gene instead of the *aphA* gene in the plasmid (Figure 3A). Glyceraldehyde 3-phosphate dehydrogenase (GapA), which catalyzes glyceraldehyde 3-phosphate to 1,3-bisphosphoglycerate, is an essential enzyme for glycolysis in *E. coli*. The knockout mutants of *gapA* cannot grow on glucose minimal media unless other carbon sources are supplemented (54,55). Two sgRNAs (sgRNA-G1 and sgRNA-G2) repressing the chromosomal *gapA* of *E. coli* were examined for their ability to inhibit cell growth in the LB or EZ media containing 25  $\mu$ g/ml of kanamycin, which was required to maintain pSLiP. When the dCas9 protein was expressed by L-rhamnose, cells in which *gapA* was repressed by the sgRNA-G1 or sgRNA-G2 showed inhibited growth in both the LB (82% or 90%) and EZ (89% or 95%) media compared to the growth of control *E. coli* cells harboring an empty plasmid (Figure 3B). The *E. coli* cells repressing *gapA* showed an optical density of less than 0.1 at 600 nm after 23 h (OD<sub>600</sub> at 23 h – OD<sub>600</sub> at 0 h) incubation in EZ medium (Figure 3C). Conversely, the control cells reached the stationary phase after 16 h. By using the CRISPRi-based inverter cascade targeting the *gapA* gene, *E. coli* cells containing three plasmids (pSLiP-G1G2, pT-GFP-rG1 and pA-RFP-rG2) were enriched in LB or EZ media with a reduced concentration of 25  $\mu$ g/ml kanamycin (Figure 3D and E).

## Stable maintenance of plasmids producing toxic metabolites

A disadvantage of antibiotics when selecting plasmids is that plasmid-free cells can outgrow plasmid-containing cells. This is due to the degradation of antibiotics by the enzymes produced by plasmid-bearing cells (56). This appears to be severe when the cells containing the plasmids show delayed growth caused by toxic proteins or metabolites produced from the transformed plasmids (47,57,58). We tested whether the cascaded logic inverter gate could overcome these issues in antibiotic-based selection. As a model system, we adopted *E. coli* cells that produced (–)- $\alpha$ -bisabolol via synthetic mevalonate (MVA) pathway encoded by a pTM-BBS (47). Previously, an *E. coli*-pTM-BBS strain was found to produce a marginal amount of (–)- $\alpha$ -bisabolol at 37°C because of the instability of the plasmid (47). For CRISPRi selection, the anti-sgRNA, sgRNA-rA2 (derepression of *aphA*), or sgRNA-rG2 (derepression of *gapA*) was inserted into the pTM-BBS (Figure 4A and B). To select and maintain the plasmids, an ampicillin-only treatment or a combination of ampicillin and the CRISPRi-based inverter cascade (dual selection) was used (Figure 4C). In contrast to that in the ampicillin-only selection, the (–)- $\alpha$ -bisabolol production increased by 3.7-fold and 6.2-fold by sgRNA-rA2 and sgRNA-rG2, respectively, under dual selection (Figure 4C). Interestingly, cell growth also showed a 1.8-fold (sgRNA-rA2) and 1.6-fold (sgRNA-rG2) increase following dual selection (Figure 4C). To probe

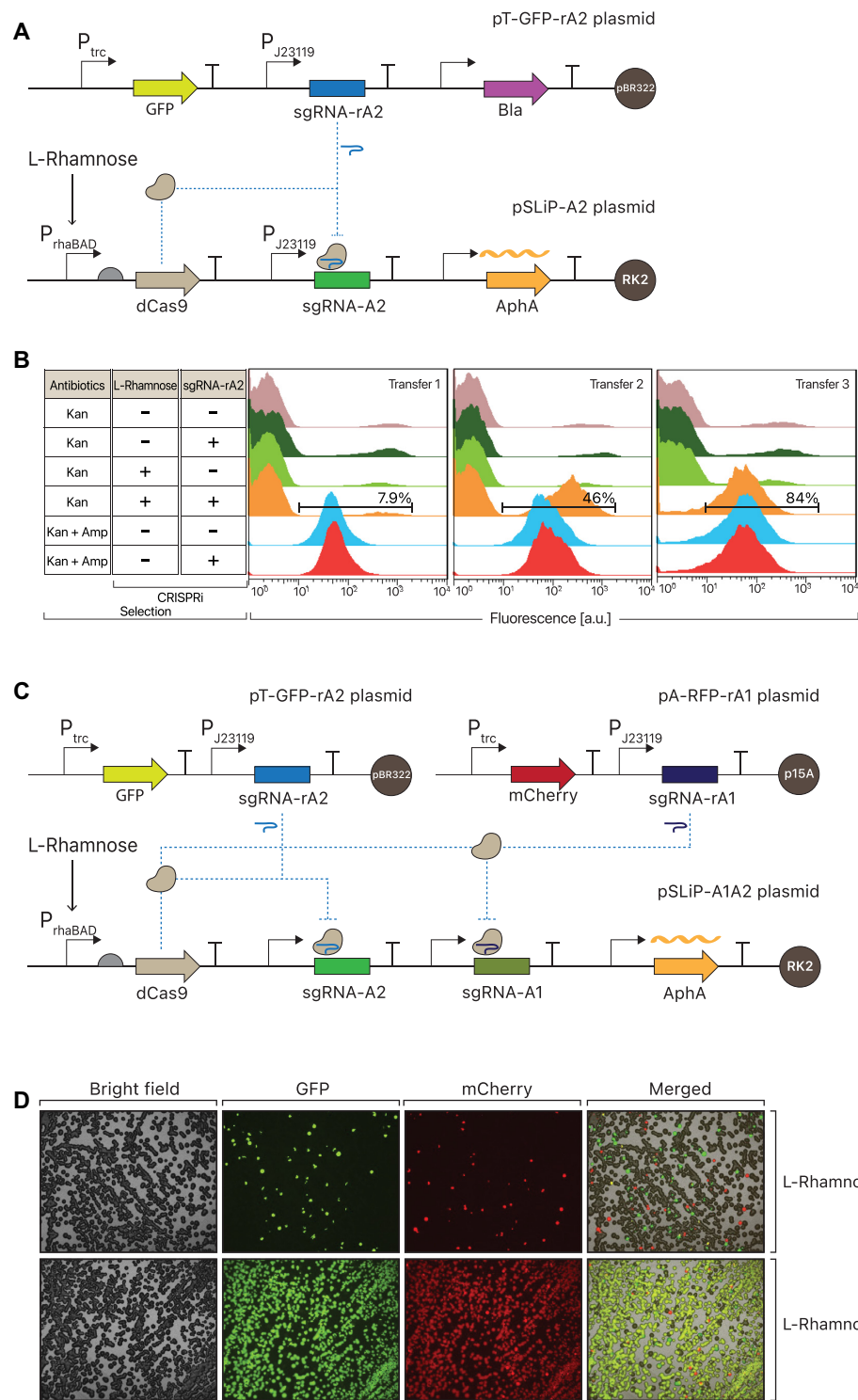


**Figure 2.** Selection and enrichment of multiple plasmids using the CRISPRi-based double inverter system repressing the expression of antibiotic-resistance genes. (A) The *gfp* gene and sgRNA-rA2 cassette were inserted into the pTrc99A plasmid, which yielded a pT-GFP-rA2 plasmid. When the pT-GFP-rA2 plasmid was introduced into the *E. coli* cells harboring pSLiP-A2, the resulting *E. coli* cells recovered their growth in the presence of 200  $\mu$ M kanamycin for CRISPRi selection as the dCas9/sgRNA-rA2 complex repressed the expression of sgRNA-A2 that targeted *aphA* repression. (B) The pT-GFP-rA2 plasmid was enriched using the pSLiP-A2 plasmid after plasmid transformation. *E. coli* cells transformed with both plasmids were cultured via serial transfers in LB medium supplemented with kanamycin and various combinations of L-rhamnose and ampicillin. For each transfer, single-cell fluorescence was determined using flow cytometry. (C) Selection of three plasmids by kanamycin alone. Two plasmids (pA-RFP-rA1 and pT-GFP-rA2) were generated and introduced into the *E. coli* cells harboring the pSLiP-A1A2 plasmid. pA-RFP-rA1 and pT-GFP-rA2 expressed mCherry and GFP, respectively. (D) *E. coli* cells transformed with three plasmids were cultured via serial transfers in LB medium with L-rhamnose and kanamycin. Following three serial transfers, *E. coli* cells were grown on the LB solid medium with L-rhamnose and kanamycin. For the negative control, *E. coli* cells with three plasmids were cultured in the absence of L-rhamnose.



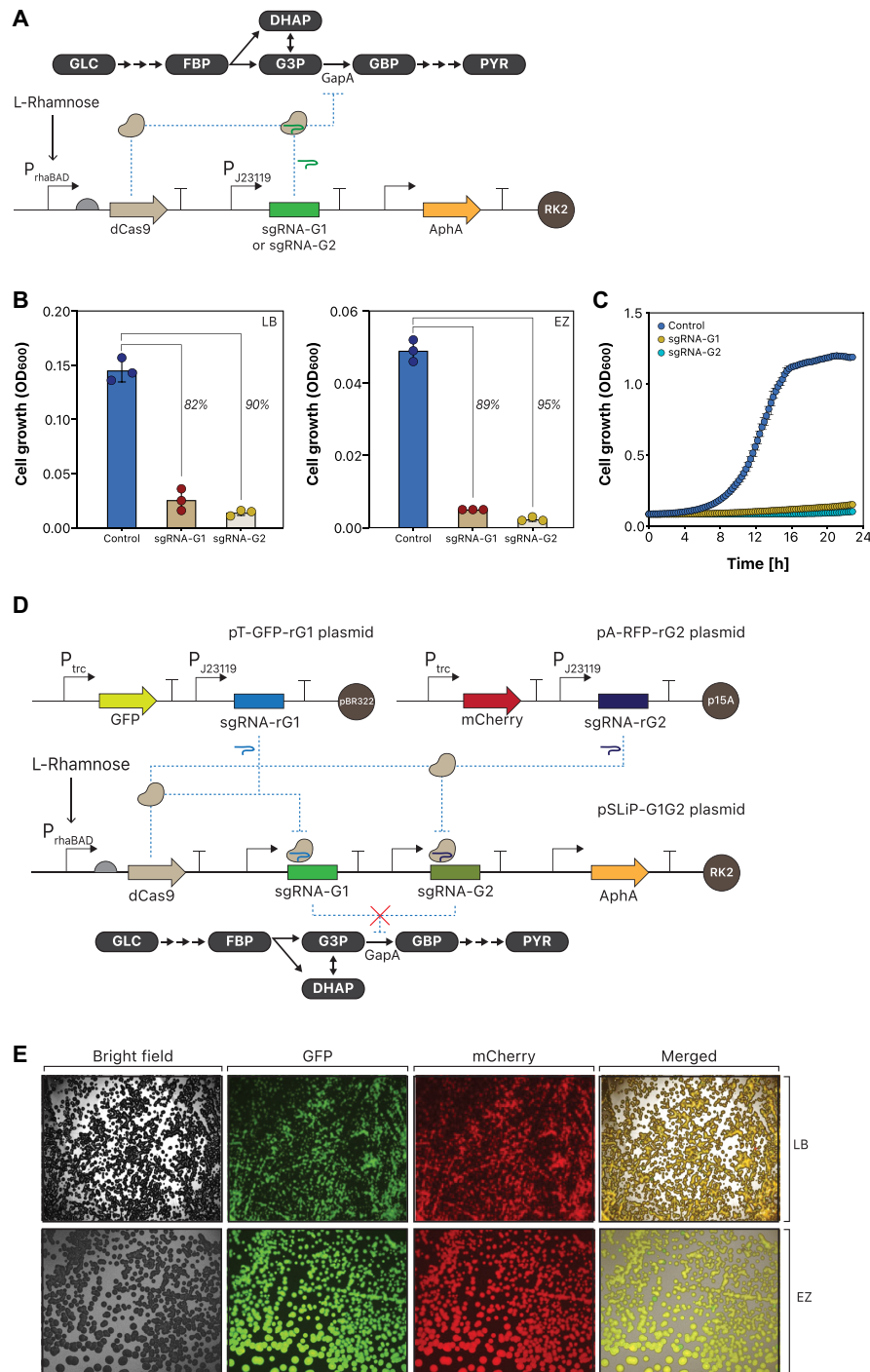


**Figure 3.** Selection and enrichment of multiple plasmids using the CRISPRi-based double inverter system repressing the expression of a cellular essential gene. (A) *E. coli gapA* gene encoding glyceraldehyde 3-phosphate dehydrogenase involved in glycolysis is essential for growing in complex or glucose minimal media. sgRNA targeting *aphA* in pSECRi was replaced with sgRNA-G1 or sgRNA-G2 that were complexed with dCas9 to inhibit the transcription of *gapA* in *E. coli* cells. (B) Two sgRNAs (sgRNA-G1 and sgRNA-G2) were designed and created to repress the expression of the *gapA* gene. A single colony of *E. coli* cells harboring pSLiP-G1 or pSLiP-G2 was inoculated and grown overnight in LB or EZ media supplemented with L-rhamnose and kanamycin. Three independent biological replicates are represented. All these four comparisons are statistically different with *p*-values <0.001 (Source Data File). (C) Three independent single colonies containing pSLiP-G1 or pSLiP-G2 plasmid were grown overnight in an EZ medium supplemented with L-rhamnose and kanamycin. A total of 1% (v/v) of cultured cells was inoculated into a fresh EZ medium in the presence of L-rhamnose and kanamycin. Cell growth was monitored using a plate reader (Infinite 200 Pro, Tecan). Three independent biological replicates are represented. The control experiment was conducted with *E. coli* cells containing the pSEVA221 plasmid. (D) Three plasmids, pT-GFP-rG1, pA-RFP-rG2, and pSLiP-G1G2, were selected in the EZ medium supplemented with only kanamycin after plasmid transformation. The pT-GFP-rG1 plasmid encoded GFP and sgRNA-rG1 which repressed sgRNA-G1. pA-RFP-rG2 expressed mCherry and sgRNA-rG2 which repressed sgRNA-G2. (E) *E. coli* cells transformed with three plasmids were grown in LB or EZ media supplemented with L-rhamnose and kanamycin. Following three serial transfers, *E. coli* cells were grown on the LB or EZ solid media with L-rhamnose and kanamycin.

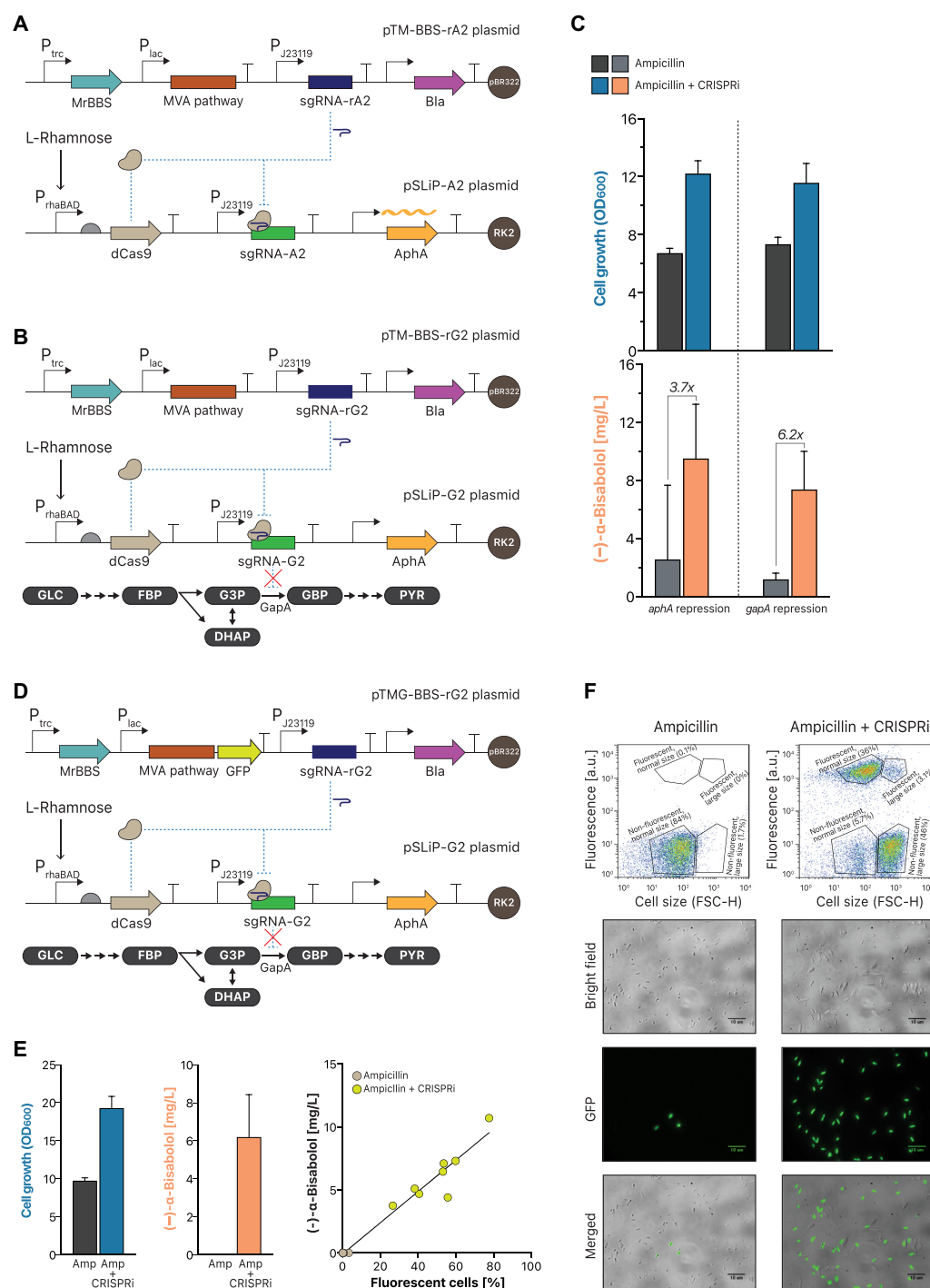


**Figure 4.** Increased production of (–)-α-bisabolol using the CRISPRi-based double inverter system. An (–)-α-bisabolol production plasmid, pTM-BBS, was used for sgRNA-rA2 or sgRNA-rG2 tagging. (A) sgRNA-rA2 repressed the expression of sgRNA-A2 which was responsible for the repression of the kanamycin-resistance gene (*aphA*). (B) sgRNA-rG2 repressed the expression of sgRNA-G2 which repressed *gapA*. (C) *E. coli* cells harboring both pTM-BBS-rA2 and pSLiP-A2 or *E. coli* cells containing both pTM-BBS-rG2 and pSLiP-G2 were grown in TBG media supplemented with ampicillin, kanamycin, and L-rhamnose. Optical density was measured to evaluate cell growth. (–)-α-Bisabolol concentrations were determined using gas chromatography. Four independent biological replicates are represented. The control experiment (antibiotics only) was conducted with *E. coli* cells containing anti-sgRNA-tagged plasmid and pSEVA221 instead of pSLiP. The *p*-values of cell growth tests were 0.037 and 0.008, respectively (Source Data File). The *p*-values of (–)-α-bisabolol production tests were < 0.001 and 0.002, respectively (Source Data File). (D) A *gfp* gene was inserted into the pTM-BBS-rG2 plasmid. (E) *E. coli* cells containing both pTMG-BBS-rG2 and pSLiP-G2 were grown in TBG media supplemented with ampicillin, kanamycin, and L-rhamnose. Optical density was measured to evaluate cell growth. (–)-α-Bisabolol concentrations were determined using gas chromatography. Single-cell fluorescence was determined using flow cytometry. Eight independent biological replicates are represented. Two-tailed *t*-tests of dual selection and ampicillin-only are all significant with *p*-values < 0.001 (Source Data File). The control experiment (Abs, antibiotics-only) was conducted with *E. coli* cells containing the anti-sgRNA-tagged plasmid and pSEVA221 instead of pSLiP. (F) Cell size and fluorescence analysis. Forward scatter (FSC-H) and GFP fluorescence (FL1-H) were analyzed using flow cytometry. Cell size and fluorescence were analyzed using a fluorescence microscope.

whether the increased production of (–)- $\alpha$ -bisabolol was caused by an increase in plasmid stability, we inserted *gfp* into pTM-BBS-rG2 to distinguish the cells containing the plasmid (Figure 4D). Consistent with the results in Figure 4C, the dual selection method yielded greater (–)- $\alpha$ -bisabolol production and cell growth than those from the ampicillin-based selection (Figure 4E). Interestingly, the *E. coli* cells harboring both pSLiP-G2 and pTMG-BBS-rG2 showed various degrees of (–)- $\alpha$ -bisabolol titers. Moreover, the production of (–)- $\alpha$ -bisabolol increased as the fluorescent *E. coli* cells increased (Figure 4E). The *E. coli* cells cultured using the dual selection method yielded greater fluorescence (27–78%,  $n = 8$ ) than those grown in ampicillin alone (Figure 4E), which showed almost no fluorescence. Of the cells without fluorescence (51.7% of the total cells), 46% were enlarged in the dual selection while 84% selected in the ampicillin-only treatment exhibited normal cell sizes (Figure 4F). The enlargement of cells may be owing to the isopentenyl pyrophosphate (IPP) toxicity. Since the pTMG-BBS-rG2 plasmid lacks the *ispA* gene encoding geranyl diphosphate/farnesyl diphosphate synthase that catalyzes the consumption of IPP to produce (–)- $\alpha$ -bisabolol, IPP accumulation would lead cell elongation along with compromised membrane integrity as previously reported (58). Overall, the CRISPRi-based inverter cascade system enabled the *E. coli* cells to stably contain the toxic plasmids, thereby leading to greater production of (–)- $\alpha$ -bisabolol.

#### Antibiotic-free production of (–)- $\alpha$ -bisabolol

To avoid the use of kanamycin for pSLiP, we used an *E. coli* auxotroph that required D-Glu for its growth. The *E. coli* WM335 strain is the only well-known D-Glu auxotrophic strain that cannot grow on a complex medium (59,60). To use this auxotrophic *E. coli* strain, a gene encoding glutamate racemase (RacE) of *Bacillus subtilis* (61) was inserted into pSLiP-G2 (pSLiP-G2-RacE), which harbored the sgRNA-G2 repressing the essential *gapA* gene (Figure 5A). Once the WM335 strain had been transformed with pSLiP-G2-RacE, its growth was monitored in the presence or absence of L-rhamnose. In the presence of L-rhamnose, the CRISPRi-based *gapA* repression resulted in a long lag phase (approximately 10 h) whereas the WM335-pSLiP-G2-RacE strain showed almost no lag phase in the absence of L-rhamnose (Figure 5B). For the analysis of the CRISPRi-based inverter cascade, we introduced pT-GFP-rG2 or pTrc99A into the WM335-pSLiP-G2-RacE strain, which yielded the WM335-pSLiP-G2-RacE/pT-GFP-rG2 or WM335-pSLiP-G2-RacE/pTrc99A strain, respectively (Figure 5C). We mixed the two strains at a 1:10 ratio (WM335-pSLiP-G2-RacE/pT-GFP-rG2: WM335-pSLiP-G2-RacE/pTrc99A) and cultured them in the presence or absence of L-rhamnose. The WM335-pSLiP-G2-RacE/pT-GFP-rG2 cells were enriched by two serial passage rounds only in the presence of L-rhamnose (Figure 5D). Given that the combined selection method using the D-Glu auxotroph and CRISPRi-based repression of the essential *gapA* gene successfully enriched the *E. coli* cells containing the two plasmids, we applied this method to produce (–)- $\alpha$ -bisabolol. We introduced the *gfp* gene and sgRNA-rG2 cassette into pTSN-Bisa-Sa which also ex-

pressed farnesyl-diphosphate synthase (IspA) for the efficient production of (–)- $\alpha$ -bisabolol (Figure 5E). The resulting plasmid, pTSNG-Bisa-Sa-rG2, was introduced into the *E. coli* WM335 strain harboring the pSLiP-G2-RacE strain. Then, the WM335-pSLiP-G2-RacE/pTSNG-Bisa-Sa-rG2 strain was cultured under four different conditions: LB medium (control), antibiotics (ampicillin), CRISPRi (L-rhamnose), and dual (antibiotics + CRISPRi) selection. The cells grown under CRISPRi alone or dual selection showed a 1.9-fold increase of (–)- $\alpha$ -bisabolol production compared to that of the cells grown in LB medium. They further showed a 1.5-fold increase of (–)- $\alpha$ -bisabolol production compared to that of the cells selected by antibiotics-only (Figure 5F). Over 90% of the cells selected by CRISPRi exhibited fluorescence whereas the proportion of fluorescent cells was low when they were selected by antibiotics (28–50%) or grown in LB medium (16–36%) (Figure 5G). However, the engineered WM335 strain selected by the CRISPRi inverter or dual selection presented a major cell population (>90%) that harbored the (–)- $\alpha$ -bisabolol production plasmid compared to that presented by the antibiotic selection (Figure 5G). Furthermore, the production of (–)- $\alpha$ -bisabolol was closely correlated with the number of fluorescent cells (Figure 5G), which showed that the CRISPRi-based double inverter system allowed the cells to stably maintain the plasmids producing (–)- $\alpha$ -bisabolol. Overall, our antibiotic-free CRISPRi-based inverter cascade system was successfully applied to stably maintain the production plasmids and improve the (–)- $\alpha$ -bisabolol titers without antibiotics.

#### D-Glutamate auxotrophic *E. coli* strains

To expand the utility of an antibiotic-free plasmid selection system using a combination of CRISPRi-based double inverter gates and D-Glu auxotrophy, we established a protocol for creating D-Glu auxotrophic *E. coli* strains other than WM335, which is currently the only *E. coli* strain that shows D-Glu auxotrophy. The *E. coli* WM335 strain contains two mutations responsible for its D-Glu auxotrophy: a single point mutation (G722A) in *murI* for the loss of glutamate racemase activity, and double mutations (G486A and G1062T) in *gltS* to increase the uptake of D-Glu (60). To confer D-Glu auxotrophy into the *E. coli* DH5 $\alpha$  strain, which has been widely used as a host in routine cloning applications, the *murI* gene of the DH5 $\alpha$  strain was replaced with a mutated *gltS* (*mgltS*) in the WM335 strain using a one-step genome engineering method (Figure 6A). The resulting mutant DH5 $\alpha$  strain could not grow on LB medium unless D-Glu was exogenously supplemented (Figure 6B). A major disadvantage of the auxotroph-based plasmid selection was that the auxotrophic strains could grow in complex media. We therefore probed the ability of the D-Glu auxotrophic *E. coli* DH5 $\alpha$  strain to grow on complex media (LB, TB, 2x YT) (Figure 6C). The D-Glu auxotrophic *E. coli* DH5 $\alpha$  strain did not grow on all tested complex media in the absence of D-Glu within 24 h ( $OD_{600} < 0.05$ ), whereas the well-known D-Glu auxotrophic *E. coli* WM335 strain grew well regardless of D-Glu in complex media, LB and TB. Using this strategy, we generated auxotrophic strains of common laboratory *E. coli* strains [BL21(DE3) and SBA01]



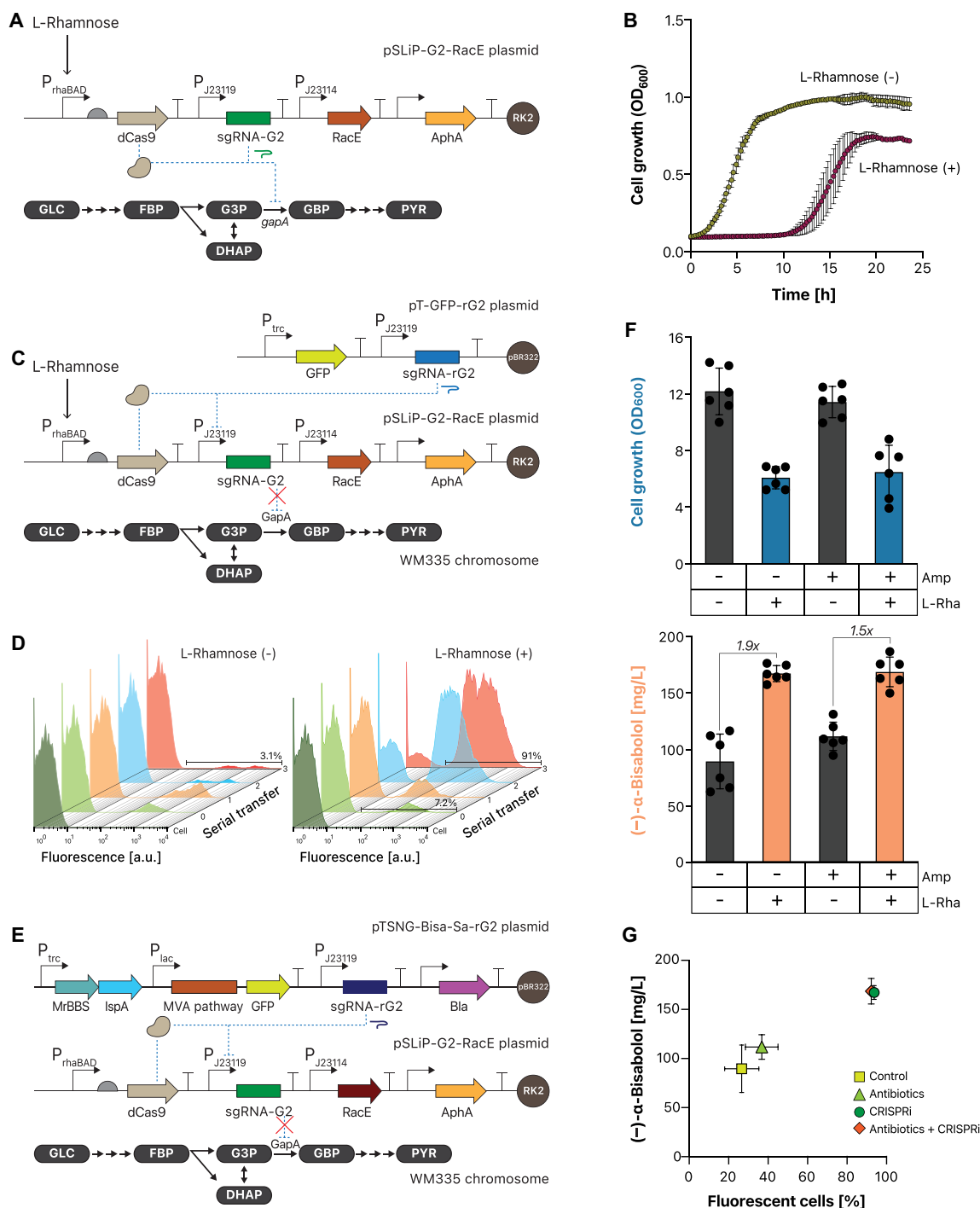


**Figure 5.** CRISPRi-based double inverter system with D-glutamate auxotrophic *E. coli* WM335. The D-glutamate auxotrophic *E. coli* WM335 strain was used to maintain two plasmids in the absence of antibiotics. (A) A gene, *racE*, encoding glutamate racemase of *Bacillus subtilis* was introduced into the pSLiP-G2 plasmid, which resulted in the pSLiP-G2-RacE plasmid. (B) WM335 strain transformed with the pSLiP-G2-RacE plasmid. Three independent biological replicates are represented. (C) WM335 cells harboring pSLiP-G2-RacE and pT-GFP-rG2 were mixed with WM335 cells harboring pSLiP-G2-RacE and pTrc99A in a 1:10 ratio. The mixed populations were cultured via serial transfer in LB medium in the absence or presence of L-rhamnose. (D) Enrichment of WM335 cells harboring pSLiP-G2-RacE and pT-GFP-rG2 by serial transfer was determined by monitoring GFP fluorescence. (E) Increased production of (-)-α-bisabolol in the WM335 strain containing the pSLiP-G2-RacE plasmid. The pTSNG-Bisa-Sa-rG2 plasmid producing (-)-α-bisabolol was introduced into the WM335 cells harboring the pSLiP-G2-RacE plasmid. This strain was grown in TBG media with various concentrations/combinations of ampicillin and L-rhamnose. (F) (-)-α-Bisabolol concentrations and cell growth were determined. Two-tailed *t*-tests (Welch two sample *t*-test) were performed to compare the growths and (-)-α-bisabolol productions of D-glutamate auxotrophic *E. coli* WM335 strain in different growth conditions of LB medium (control), antibiotics (ampicillin), CRISPRi (L-rhamnose), and dual (antibiotics + CRISPRi). *p*-values are all less than 0.001 (Source Data File), which means the growth and (-)-α-bisabolol production in CRISPRi condition is significantly different from those in the absence of CRISPRi activity (Source Data File). (G) Single-cell fluorescence was determined using flow cytometry. Correlations between (-)-α-bisabolol production and fluorescent population. Six independent biological replicates are represented.

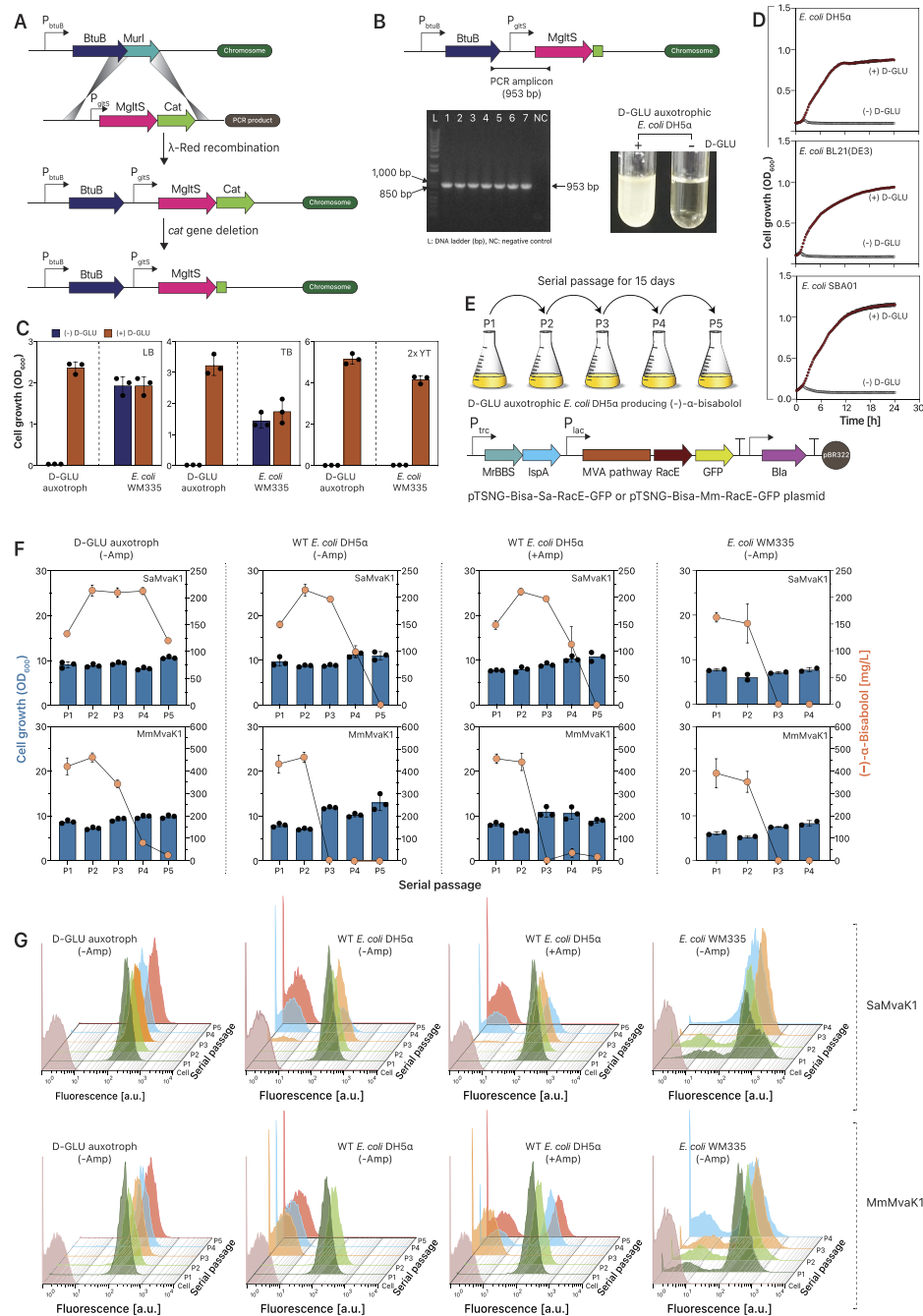


**Figure 6.** Functional characterization of D-glutamate auxotrophic *E. coli* strains. **(A)** One-step genome engineering for the construction of the D-glutamate auxotrophic *E. coli* strain. The endogenous *murI* gene was replaced by the PCR product which contained the *mgtS* gene with its promoter and the chloramphenicol resistance gene. The chloramphenicol resistance gene was removed by flippase. WT *gltS* was present in the *E. coli* DH5 $\alpha$  genome, although it is not shown here. **(B)** Verification of the D-glutamate auxotrophic *E. coli* DH5 $\alpha$  strain. Colony PCR was performed to identify positive recombinant mutants which generate 953 bp PCR amplicons. L, DNA ladder, NC, negative control (WT *E. coli* DH5 $\alpha$ ). D-Glutamate auxotrophy of the recombinant strain was confirmed via cultivation in LB medium or LB medium supplemented with D-glutamate. **(C)** Cell growth of the D-glutamate auxotrophic *E. coli* DH5 $\alpha$  in complex media. D-Glutamate auxotrophic *E. coli* DH5 $\alpha$  or *E. coli* WM335 strain was grown in LB, TB, or 2x YT medium. Data represent averages from three independent biological replicates. Error bars show standard deviation. Two-tailed *t*-tests were performed to compare the cell growths of D-glutamate auxotrophic *E. coli* DH5 $\alpha$  and *E. coli* WM335 strains in LB, TB, and 2x YT media. The growth of D-glutamate auxotrophic *E. coli* DH5 $\alpha$  with D-glutamate is significantly different from the conditions without D-glutamate with *p*-values <0.001 in all media. However, the *t*-tests of D-glutamate auxotrophic *E. coli* WM335 strain are not significant in LB and TB media with *p*-values of 0.313 and 0.422, respectively (Source Data File). **(D)** Cell growth of the D-glutamate auxotrophic *E. coli* DH5 $\alpha$ , BL21(DE3), and SBA01 strains in LB medium. Data represent averages from three independent biological replicates. Error bars show standard deviation. **(E)** Antibiotic-free (–)- $\alpha$ -bisabolol production for 15 days. Cell growth and (–)- $\alpha$ -bisabolol concentration were determined during the long-term cultivation. Data represent averages of three independent biological replicates. Error bars show standard deviation. **(F)** Single-cell fluorescence was determined during the long-term cultivation using flow cytometry. Two different mevalonate kinase (MvaK1) enzymes were examined: SaMvaK1, *Staphylococcus aureus* MvaK1; MmMvaK1, *Methanosarcina mazei* MvaK1. **(G)** Stability of pTSNG-Bisa-Sa-RacE-GFP or pTSNG-Bisa-Mm-RacE-GFP plasmid in different *E. coli* cells during the serial transfer was determined by monitoring GFP fluorescence.

with D-Glu auxotrophy that are useful for recombinant protein expression and biochemical production (Figure 6D) (62). By using the D-Glu auxotrophic *E. coli* DH5 $\alpha$  strain, (–)- $\alpha$ -bisabolol was produced. A plasmid, pTSNG-Bisa-Sa-RacE, was created by introducing *racE* and *gfp* into pTSN-Bisa-Sa (Figure 6E). The D-Glu auxotrophic *E. coli* DH5 $\alpha$ , WT *E. coli* DH5 $\alpha$ , and *E. coli* WM335 strains harboring pTSNG-Bisa-Sa-RacE were cultured for 15 days through serial passages to monitor the cell growth, (–)- $\alpha$ -bisabolol production (Figure 6F), and plasmid stability based on fluorescence (Figure 6E). The D-Glu auxotrophic DH5 $\alpha$  strain stably produced (–)- $\alpha$ -bisabolol for four serial transfers (P1–P4) in the ampicillin-free medium, although (–)- $\alpha$ -bisabolol production decreased by 44% in P5 compared to that in P2–P4 (Figure 6F). The D-Glu auxotrophic DH5 $\alpha$  strain showed approximately 100% plasmid stability with homogenous GFP expression for 15 days (P1–P5, Figure 6G). In contrast, the (–)- $\alpha$ -bisabolol production of the WT *E. coli* DH5 $\alpha$  strain rapidly decreased in P4 cultivation, and (–)- $\alpha$ -bisabolol was not produced in P5 in the absence of ampicillin. This decreased (–)- $\alpha$ -bisabolol production was highly correlated with the rapid loss of pTSNG-Bisa-Sa-RacE from the P3 cultivation (Figure 6G). Interestingly, similar results regarding (–)- $\alpha$ -bisabolol production and plasmid stability were observed in the presence of ampicillin. The WM335 strain containing pTSNG-Bisa-Sa-RacE showed colonial variations in (–)- $\alpha$ -bisabolol production and unstable plasmid maintenance (Figures 6F and G). To examine the applicability of the D-Glu auxotrophic *E. coli* strain in a more toxic environment, the MvaK1 enzyme of *Staphylococcus aureus* in the MVA pathway of pTSNG-Bisa-Sa-RacE was replaced with MvaK1 (MmMvaK1), which has been used to improve the flux of the MVA pathway and the production of (–)- $\alpha$ -bisabolol (63). The resulting plasmid, pTSNG-Bisa-Mm-RacE, in the D-Glu auxotrophic *E. coli* DH $\alpha$  strain showed an increased production of (–)- $\alpha$ -bisabolol that was over twice as high as that in the same strain with pTSNG-Bisa-Sa-RacE (Figure 6F). The production of (–)- $\alpha$ -bisabolol, however, rapidly decreased at P3, although the plasmid was stably maintained (Figure 6G). The decrease of (–)- $\alpha$ -bisabolol production was more remarkable in the WT *E. coli* DH $\alpha$  strain, which did not show a production of (–)- $\alpha$ -bisabolol regardless of antibiotics. The WT *E. coli* DH $\alpha$  strain completely lost the plasmid in the P3 cultivation, although the strain harbouring the plasmid re-emerged in the presence of antibiotics and produced a marginal amount of (–)- $\alpha$ -bisabolol in the P4 cultivation. The WM335 strain with the same plasmid showed large colonial differences in the production of (–)- $\alpha$ -bisabolol and showed highly heterogeneous fluorescent patterns during the serial passages, although most of the cells were fluorescent until the P4 cultivation. Overall, the developed D-Glu auxotrophic selection outperformed the antibiotics, addressed the instability of the plasmid, and increased (–)- $\alpha$ -bisabolol production.

Using the D-Glu auxotrophic *E. coli* DH5 $\alpha$  strain and CRISPRi-based inverter cascade, we tried to build a recombinant plasmid that is free of an antibiotic-resistance gene (*bla*). Two DNA fragments containing GFP expression cassettes and the sgRNA-tag were assembled and transformed into the D-Glu auxotrophic *E. coli* DH5 $\alpha$  harbor-

ing the pSLiP-G2-RacE plasmid. CRISPRi selection was conducted by three serial transfers in LB medium supplemented with L-rhamnose (Supplementary Figure 2). Initially, the population of D-Glu auxotrophic DH5 $\alpha$  strain transformed with the GFP plasmid was very low (0.11%) but it gradually increased and reached 85.7% after three serial cultures (Supplementary Figure 2). The *E. coli* cells containing the GFP plasmid were not enriched during serial cultures in the absence of L-rhamnose (Supplementary Figure 3). Twelve colonies from the final culture (transfer 3) were isolated and used for purification of the GFP plasmid. In agreement with flow cytometry analysis, 11 out of 12 colonies contained the GFP plasmid with the correct DNA sequence (Supplementary Figure 4), and the sgRNA-G2 cassette was correctly incorporated into the GFP plasmid instead of the *bla* gene (Supplementary Figure 5 and 6). Overall, we developed various D-Glu auxotrophic strains that are widely applicable for the production of therapeutic plasmids, recombinant proteins, and biochemicals without the use of antibiotics and antibiotic-resistance genes.

## DISCUSSION

One goal of synthetic biology is to create rational designs of new and complex biological functions using the genetic circuits that interconnect different logic gates to process multiple input signals. TFs and plasmids are widely used to create genetic circuits with increasing complexity to provide logic modules in engineered cells. Some of the major issues of building complex genetic circuits with TFs and plasmids are the limited availability of orthogonal TFs and the continuous use of different antibiotics, respectively. Compared with widely used TFs, the CRISPRi module provides an easy way to program sgRNAs to repress the expression of any gene of interest, given a PAM that is required for its function (18,19). We addressed the aforementioned issues by using the intrinsic modularity and orthogonality of CRISPRi.

We developed a CRISPRi-based plasmid selection system by building a cascaded logic inverter that mimicked the natural regulation between antibiotics and antibiotic-resistance genes. To this end, we first constructed a plasmid containing a sgRNA landing pad (pSLiP). The sgRNA expressed by the pSLiP formed a complex with dCas9 to inhibit the expression of antibiotic-resistance genes. pSLiP also allowed another sgRNA, which was encoded by another plasmid with no antibiotic-resistance genes, to bind the PAM in the promoter of the sgRNA repressing the expression of antibiotic-resistance genes. This led to the restoration of cell growth. Thus, if bacterial cells harbor pSLiP, the engineered cells can possess another plasmid in the presence of only one antibiotic that is necessary to maintain the pSLiP plasmid. Given the modularity and orthogonality of sgRNA, the CRISPRi-based selection system has the potential to expand its application to the selection of cells harboring multiple plasmids using a single selection marker in contrast to the antibiotic-based selection that requires different antibiotics. Indeed, *E. coli* cells with three plasmids were successfully selected using a single antibiotic using a multilayered CRISPRi inverter cascade. Although the multiplicity of the CRISPRi-based selection system is not limited, it should be considered that the replication ori-



gin of the plasmid is limited and that sharing the CRISPRi apparatus in several plasmids may cause a reduced repression efficiency (21,64,65). Indeed, two plasmids containing the same replication origin were not simultaneously selected using CRISPRi or antibiotic selection (Supplementary Figure 7).

The CRISPRi-based selection system can target any gene of the microbial genome because of the versatility of designing and building sgRNA. We first selected an antibiotic-resistance gene to increase antibiotic susceptibility and then replaced it with the essential gene (*gapA*) as the repression target gene of CRISPRi to ease antibiotic use. However, any essential gene can be a target gene for CRISPRi, which makes it possible to maintain multiple plasmids by repressing one essential gene or a combination of different essential genes by multiplex CRISPRi. While previously reported antibiotic-free plasmid selection systems have usually worked in defined minimal media, the CRISPRi-based selection system works well in complex media if the essential gene is properly selected as the target of sgRNAs. Although we built pSLiP using antibiotic selection (*aphA*) or host essential (*gapA*) genes in *E. coli*, our system can easily be applied to other organisms with a simple design, high efficiency, and success rate of functional CRISPRi, especially if the replication origin is available.

Replacement of the antibiotic-resistance gene with the small sgRNA cassette (~140 bp) in the CRISPRi-based selection system is attractive for the development of therapeutic plasmids. This is because it can be used to strictly maintain the production of therapeutic plasmids for higher titers and reduce costs by antibiotic-free fermentation. The sgRNA-tag, which is much smaller than antibiotic-resistance genes, can significantly reduce the plasmid size for therapeutics. Small plasmids can reduce the metabolic load of host cells by the antibiotic-resistance gene, increase the productivity of the plasmid (66), be more stable in the bacterial host, and prevent epigenetic changes in mammalian cells (36). crRNA, instead of sgRNA, can further reduce the size of plasmids (67) and adds 100 bp or less to the plasmid if a Cpf1 effector is used since it does not require a tracrRNA (68,69). However, if using another type of CRISPR system, independent examination is required.

To develop the CRISPRi-based selection system without using antibiotics, a method to select the pSLiP was required. We created a novel D-Glu auxotrophic *E. coli* strains. The D-Glu auxotrophic *E. coli* strains showing disrupted cell wall synthesis could not grow in complex media, which made the D-Glu auxotrophic selection in complex media possible. By using the D-Glu auxotrophic *E. coli* DH5 $\alpha$  strain, the production of (–)- $\alpha$ -bisabolol increased in complex media, suggesting that the CRISPRi-based selection system with D-Glu auxotrophy would be useful in producing molecules of interest in industrial fermentation without using antibiotics. In the antibiotic-based selection method, the cells without a plasmid rapidly became dominant when the plasmid expressed toxic proteins or metabolites. In this study, the *E. coli* strain that produced (–)- $\alpha$ -bisabolol lost the production plasmid during the culture. The MVA pathway responsible for (–)- $\alpha$ -bisabolol production requires a balanced expression of each enzyme because of the potential production of toxic intermediates, such as HMG-CoA

and IPP (70,71). Thus, un-optimized plasmid or culture conditions induce plasmid instability during fermentation, which yields reduced terpenoid production (47,72). Even under this condition, the CRISPRi-based selection system forced only the cells containing the (–)- $\alpha$ -bisabolol production plasmid to grow, which led to enhanced production of (–)- $\alpha$ -bisabolol during cultivation.

Plasmid copy number can vary depending on the selection conditions. The CRISPRi-based selection system does not affect the target plasmid copy number compared to antibiotic selection (Supplementary Figure 8a). The CRISPRi-based double inverter circuit is also successful in a D-Glu auxotrophic *E. coli* BL21(DE3) strain, which has been widely used to produce heterologous proteins (Supplementary Figure 8b). However, the protein production capacity of the D-Glu auxotrophic *E. coli* BL21(DE3) using the CRISPRi-based inverter cascade can be further examined with a proper model protein to demonstrate the system robustness.

Our CRISPRi-based plasmid selection system has some drawbacks to be considered. It requires the pre-induction of the dCas9 protein in pSLiP to inhibit host cell growth in contrast to antibiotics that provide immediate selection pressure. When seed culture was not induced by L-rhamnose, the CRISPRi-mediated growth inhibition was not observed in subsequent main cultures. This is presumably because it takes longer to inhibit the transcription of target genes (e.g. *aphA*, *gapA*) by the expression of the dCas9 protein and the target protein must then be removed by degradation or dilution along with cell divisions. The CRISPRi-based double inverter system can be further improved by replacing the  $P_{rhaBAD}$  promoter of the dCas9 protein with other inducer independent promoters to mitigate the dependency on L-rhamnose and increased homogenous expression of dCas9. Importantly, the CRISPRi system is more susceptible to genetic mutations than the antibiotic-based system. For the CRISPR system, the escapers emerged with an average frequency of an order of  $10^{-4}$  (73). In our case, we successfully enriched 0.11% cells which is above the general escaper frequency (Supplementary Figure 2); however, some nonfluorescent cells (~14%) were also present. Furthermore, we found that 1 out of 12 colonies did not possess the target plasmid (Supplementary Figure 4), which might be the escaper considering the escaper frequency (an order of  $10^{-4}$ ). For multiplex sgRNAs, homologous recombination between sgRNAs can cause spontaneous deletion of the sgRNA cassette. To reduce the deletion problem, it is recommended to build the pSLiP plasmid having nonrepetitive sgRNAs using the extra-long sgRNA arrays (74).

In conclusion, we developed an antibiotic-free plasmid selection system using CRISPRi and D-Glu auxotrophic *E. coli*. This system will be useful for production of bioproducts including therapeutic proteins, biochemicals, and plasmids without utilizing antibiotics.

## DATA AVAILABILITY

Data from all figures are provided in the Source Data File. A subset of the plasmids constructed in this study are available from Addgene. Individual Addgene plasmids numbers

are listed below. pSLiP-G1 (Addgene #188963), pSLiP-G2 (Addgene #188964), pSLiP-G1G2 (Addgene #188965), pSLiP-G2-RacE (Addgene #188966), pT-GFP-rG1 (Addgene #188967), pT-GFP-rG2 (Addgene #188968), pA-RFP-rG2 (Addgene #188969).

## SUPPLEMENTARY DATA

Supplementary Data are available at NAR Online.

## ACKNOWLEDGEMENTS

The authors would like to thank the members of the Synthetic Biology Research Group for valuable advice and suggestions. We also appreciated the sharing of the pSEVA plasmids from Dr. Víctor de Lorenzo at Center for National Biotechnology, CSIC, Madrid, Spain.

## FUNDING

Bio & Medical Technology Development Program [2018M3A9H3024746, 2021M3A9I4022731] of the National Research Foundation funded by the Ministry of Science and ICT of the Republic of Korea; KRIBB Research Initiative Program [KGM5402221]. Funding for open access charge: National Research Foundation funded by the Ministry of Science and ICT of the Republic of Korea.

*Conflict of interest statement.* None declared.

## REFERENCES

- Xia, P.F., Ling, H., Foo, J.L. and Chang, M.W. (2019) Synthetic genetic circuits for programmable biological functionalities. *Biotechnol. Adv.*, **37**, 107393.
- Saltepe, B., Kehribar, E.Ş., Su Yirmibeşoğlu, S.S. and Şafak Şeker, U.Ö. (2018) Cellular biosensors with engineered genetic circuits. *ACS Sens.*, **3**, 13–26.
- Xie, M. and Fussenegger, M. (2018) Designing cell function: assembly of synthetic gene circuits for cell biology applications. *Nat. Rev. Mol. Cell Biol.*, **19**, 507–525.
- Kitada, T., DiAndreth, B., Teague, B. and Weiss, R. (2018) Programming gene and engineered-cell therapies with synthetic biology. *Science*, **359**, eaad1067.
- Gao, C., Xu, P., Ye, C., Chen, X. and Liu, L. (2019) Genetic circuit-assisted smart microbial engineering. *Trends Microbiol.*, **27**, 1011–1024.
- McNerney, M.P., Doiron, K.E., Ng, T.L., Chang, T.Z. and Silver, P.A. (2021) Theranostic cells: emerging clinical applications of synthetic biology. *Nat. Rev. Genet.*, **22**, 730–746.
- Riglar, D.T. and Silver, P.A. (2018) Engineering bacteria for diagnostic and therapeutic applications. *Nat. Rev. Microbiol.*, **16**, 214–225.
- Charbonneau, M.R., Isabella, V.M., Li, N. and Kurtz, C.B. (2020) Developing a new class of engineered live bacterial therapeutics to treat human diseases. *Nat. Commun.*, **11**, 1738.
- Cubillos-Ruiz, A., Guo, T., Sokolovska, A., Miller, P.F., Collins, J.J., Lu, T.K. and Lora, J.M. (2021) Engineering living therapeutics with synthetic biology. *Nat. Rev. Drug Discov.*, **20**, 941–960.
- Chen, Y., Zhang, S., Young, E.M., Jones, T.S., Densmore, D. and Voigt, C.A. (2020) Genetic circuit design automation for yeast. *Nat. Microbiol.*, **5**, 1349–1360.
- Cheng, F., Tang, X.L. and Kardashliev, T. (2018) Transcription factor-based biosensors in high-throughput screening: advances and applications. *Biotechnol. J.*, **13**, e1700648.
- Xiang, Y., Dalchau, N. and Wang, B. (2018) Scaling up genetic circuit design for cellular computing: advances and prospects. *Nat. Comput.*, **17**, 833–853.
- Jones, T.S., Oliveira, S.M.D., Myers, C.J., Voigt, C.A. and Densmore, D. (2022) Genetic circuit design automation with Cello 2.0. *Nat. Protoc.*, **17**, 1097–1113.
- Taketani, M., Zhang, J., Zhang, S., Triassi, A.J., Huang, Y.-J., Griffith, L.G. and Voigt, C.A. (2020) Genetic circuit design automation for the gut resident species *Bacteroides thetaiotaomicron*. *Nat. Biotechnol.*, **38**, 962–969.
- Nielsen, A.A., Der Bryan, S., Shin, J., Vaidyanathan, P., Paralanov, V., Strychalski Elizabeth, A., Ross, D., Densmore, D. and Voigt, Christopher, A. (2016) Genetic circuit design automation. *Science*, **352**, aac7341.
- Taylor, N.D., Garruss, A.S., Moretti, R., Chan, S., Arbing, M.A., Cascio, D., Rogers, J.K., Isaacs, F.J., Kosuri, S., Baker, D. et al. (2016) Engineering an allosteric transcription factor to respond to new ligands. *Nat. Methods*, **13**, 177–183.
- Feng, J., Jester, B.W., Tinberg, C.E., Mandell, D.J., Antunes, M.S., Chari, R., Morey, K.J., Rios, X., Medford, J.I., Church, G.M. et al. (2015) A general strategy to construct small molecule biosensors in eukaryotes. *Elife*, **4**, e10606.
- Qi, L.S., Larson, M.H., Gilbert, L.A., Doudna, J.A., Weissman, J.S., Arkin, A.P. and Lim, W.A. (2013) Repurposing CRISPR as an RNA-guided platform for sequence-specific control of gene expression. *Cell*, **152**, 1173–1183.
- Bikard, D., Jiang, W., Samai, P., Hochschild, A., Zhang, F. and Marraffini, L.A. (2013) Programmable repression and activation of bacterial gene expression using an engineered CRISPR-Cas system. *Nucleic Acids Res.*, **41**, 7429–7437.
- Perez-Pinera, P., Kocak, D.D., Vockley, C.M., Adler, A.F., Kabadi, A.M., Polstein, L.R., Thakore, P.I., Glass, K.A., Ousterout, D.G., Leong, K.W. et al. (2013) RNA-guided gene activation by CRISPR-Cas9-based transcription factors. *Nat. Methods*, **10**, 973–976.
- Zhang, S. and Voigt, C.A. (2018) Engineered dCas9 with reduced toxicity in bacteria: implications for genetic circuit design. *Nucleic Acids Res.*, **46**, 11115–11125.
- Santos-Moreno, J. and Schaeferli, Y. (2020) CRISPR-based gene expression control for synthetic gene circuits. *Biochem. Soc. Trans.*, **48**, 1979–1993.
- Wu, F., Shim, J., Gong, T. and Tan, C. (2020) Orthogonal tuning of gene expression noise using CRISPR–Cas. *Nucleic Acids Res.*, **48**, e76.
- McCarty, N.S., Graham, A.E., Studená, L. and Ledesma-Amaro, R. (2020) Multiplexed CRISPR technologies for gene editing and transcriptional regulation. *Nat. Commun.*, **11**, 1281.
- Liu, Y., Zeng, Y., Liu, L., Zhuang, C., Fu, X., Huang, W. and Cai, Z. (2014) Synthesizing AND gate genetic circuits based on CRISPR-Cas9 for identification of bladder cancer cells. *Nat. Commun.*, **5**, 5393.
- Gander, M.W., Vrana, J.D., Voje, W.E., Carothers, J.M. and Klavins, E. (2017) Digital logic circuits in yeast with CRISPR-dCas9 NOR gates. *Nat. Commun.*, **8**, 15459.
- Kim, H., Bojar, D. and Fussenegger, M. (2019) A CRISPR/Cas9-based central processing unit to program complex logic computation in human cells. *Proc. Natl. Acad. Sci. U.S.A.*, **116**, 7214–7219.
- Hofmann, A., Falk, J., Prangemeier, T., Happel, D., Köber, A., Christmann, A., Koepl, H. and Kolmar, H. (2019) A tightly regulated and adjustable CRISPR-dCas9 based AND gate in yeast. *Nucleic Acids Res.*, **47**, 509–520.
- Fan, J., Liu, Y., Liu, L., Huang, Y., Li, X. and Huang, W. (2020) A multifunction lipid-based CRISPR-Cas13a genetic circuit delivery system for bladder cancer gene therapy. *ACS Synth. Biol.*, **9**, 343–355.
- Li, Z., Rosenbaum, M.A., Venkataraman, A., Tam, T.K., Katz, E. and Angenent, L.T. (2011) Bacteria-based AND logic gate: a decision-making and self-powered biosensor. *Chem. Commun.*, **47**, 3060–3062.
- Nielsen, A.A. and Voigt, C.A. (2014) Multi-input CRISPR/Cas genetic circuits that interface host regulatory networks. *Mol. Syst. Biol.*, **10**, 763–763.
- Barbier, I., Perez-Carrasco, R. and Schaeferli, Y. (2020) Controlling spatiotemporal pattern formation in a concentration gradient with a synthetic toggle switch. *Mol. Syst. Biol.*, **16**, e9361.
- Zorzan, I., López, A.R., Malysheva, A., Ellis, T. and Barberis, M. (2021) Synthetic designs regulating cellular transitions: fine-tuning of switches and oscillators. *Curr. Opin. Syst. Biol.*, **25**, 11–26.

34. Mansouri, M., Strittmatter, T. and Fussenegger, M. (2019) Light-controlled mammalian cells and their therapeutic applications in synthetic biology. *Adv. Sci. (Weinh)*, **6**, 1800952.
35. Mignon, C., Sodoyer, R. and Werle, B. (2015) Antibiotic-free selection in biotherapeutics: now and forever. *Pathogens*, **4**, 157–181.
36. Oliveira, P.H. and Mairhofer, J. (2013) Marker-free plasmids for biotechnological applications – implications and perspectives. *Trends Biotechnol.*, **31**, 539–547.
37. Wright, O., Stan, G.B. and Ellis, T. (2013) Building-in biosafety for synthetic biology. *Microbiology (Reading)*, **159**, 1221–1235.
38. Weigel, L.M., Clewell, D.B., Gill, S.R., Clark, N.C., McDougal, L.K., Flannagan, S.E., Kolonay, J.F., Shetty, J., Killgore, G.E. and Tenover, F.C. (2003) Genetic analysis of a high-level vancomycin-resistant isolate of *Staphylococcus aureus*. *Science*, **302**, 1569–1571.
39. Robertson, J.S. and Griffiths, E. (2006) In: Saltzman, W.M., Shen, H. and Brandsma, J.L. (eds) *DNA Vaccines: Methods and Protocols*. Humana Press, Totowa, NJ, pp. 363–374.
40. Smith, M.A. and Bidochka, M.J. (1998) Bacterial fitness and plasmid loss: the importance of culture conditions and plasmid size. *Can. J. Microbiol.*, **44**, 351–355.
41. Saleski, T.E., Chung, M.T., Carruthers, D.N., Khasbaatar, A., Kurabayashi, K. and Lin, X.N. (2021) Optimized gene expression from bacterial chromosome by high-throughput integration and screening. *Sci. Adv.*, **7**, eabe1767.
42. Goyal, G., Costello, Z., Alonso-Gutierrez, J., Kang, A., Lee, T.S., Garcia Martin, H. and Hillson, N.J. (2018) Parallel integration and chromosomal expansion of metabolic pathways. *ACS Synth. Biol.*, **7**, 2566–2576.
43. Vandermeulen, G., Marie, C., Scherman, D. and Préat, V. (2011) New generation of plasmid backbones devoid of antibiotic resistance marker for gene therapy trials. *Mol. Ther.*, **19**, 1942–1949.
44. Williams, S.G., Cranenburgh, R.M., Weiss, A.M.E., Wrighton, C.J., Hanak, J.A.J. and Sherratt, D.J. (1998) Repressor titration: a novel system for selection and stable maintenance of recombinant plasmids. *Nucleic Acids Res.*, **26**, 2120–2124.
45. Dong, W.R., Xiang, L.X. and Shao, J.Z. (2010) Novel antibiotic-free plasmid selection system based on complementation of host auxotrophy in the NAD *de novo* synthesis pathway. *Appl. Environ. Microbiol.*, **76**, 2295–2303.
46. Schmidt, C.M., Shis, D.L., Nguyen-Huu, T.D. and Bennett, M.R. (2012) Stable maintenance of multiple plasmids in *E. coli* using a single selective marker. *ACS Synth. Biol.*, **1**, 445–450.
47. Kim, S.K., Han, G.H., Seong, W., Kim, H., Kim, S.W., Lee, D.H. and Lee, S.G. (2016) CRISPR interference-guided balancing of a biosynthetic mevalonate pathway increases terpenoid production. *Metab. Eng.*, **38**, 228–240.
48. Datsenko, K.A. and Wanner, B.L. (2000) One-step inactivation of chromosomal genes in *Escherichia coli* K-12 using PCR products. *Proc. Natl. Acad. Sci. U.S.A.*, **97**, 6640–6645.
49. Reynolds, P.E. (1989) Structure, biochemistry and mechanism of action of glycopeptide antibiotics. *Eur. J. Clin. Microbiol. Infect. Dis.*, **8**, 943–950.
50. Wise, R. (1999) A review of the mechanisms of action and resistance of antimicrobial agents. *Can. Respir. J.*, **6**, 20A–22A.
51. Davies, J. and Davies, D. (2010) Origins and evolution of antibiotic resistance. *Microbiol. Mol. Biol. Rev.*, **74**, 417–433.
52. Cho, S., Choe, D., Lee, E., Kim, S.C., Palsson, B. and Cho, B.K. (2018) High-level dCas9 expression induces abnormal cell morphology in *Escherichia coli*. *ACS Synth. Biol.*, **7**, 1085–1094.
53. Nurizzo, D., Shewry, S.C., Perlin, M.H., Brown, S.A., Dholakia, J.N., Fuchs, R.L., Deva, T., Baker, E.N. and Smith, C.A. (2003) The crystal structure of aminoglycoside-3'-phosphotransferase-IIa, an enzyme responsible for antibiotic resistance. *J. Mol. Biol.*, **327**, 491–506.
54. Seta, F.D., Boschi-Muller, S., Vignais, M.L. and Branlant, G. (1997) Characterization of *Escherichia coli* strains with *gapA* and *gapB* genes deleted. *J. Bacteriol.*, **179**, 5218–5221.
55. Hillman, J.D. and Fraenkel, D.G. (1975) Glyceraldehyde 3-phosphate dehydrogenase mutants of *Escherichia coli*. *J. Bacteriol.*, **122**, 1175–1179.
56. Korpimäki, T., Kurittu, J. and Karp, M. (2003) Surprisingly fast disappearance of  $\beta$ -lactam selection pressure in cultivation as detected with novel biosensing approaches. *J. Microbiol. Methods*, **53**, 37–42.
57. Dumon-Seignover, L., Cariot, G. and Vuillard, L. (2004) The toxicity of recombinant proteins in *Escherichia coli*: a comparison of overexpression in BL21(DE3), C41(DE3), and C43(DE3). *Protein Expr. Purif.*, **37**, 203–206.
58. George, K.W., Thompson, M.G., Kim, J., Baidoo, E.E.K., Wang, G., Benites, V.T., Petzold, C.J., Chan, L.J.G., Yilmaz, S., Turhanen, P. et al. (2018) Integrated analysis of isopentenyl pyrophosphate (IPP) toxicity in isoprenoid-producing *Escherichia coli*. *Metab. Eng.*, **47**, 60–72.
59. Lugtenberg, E.J., Wijsman, H.J. and van Zaane, D. (1973) Properties of a D-glutamic acid-requiring mutant of *Escherichia coli*. *J. Bacteriol.*, **114**, 499–506.
60. Dougherty, T.J., Thanassi, J.A. and Pucci, M.J. (1993) The *Escherichia coli* mutant requiring D-glutamic acid is the result of mutations in two distinct genetic loci. *J. Bacteriol.*, **175**, 111–116.
61. Ashiuchi, M., Tani, K., Soda, K. and Misono, H. (1998) Properties of glutamate racemase from *Bacillus subtilis* IFO 3336 producing poly- $\gamma$ -glutamate. *J. Biochem.*, **123**, 1156–1163.
62. Seong, W., Han, G.H., Lim, H.S., Baek, J.I., Kim, S.J., Kim, D., Kim, S.K., Lee, H., Kim, H., Lee, S.G. et al. (2020) Adaptive laboratory evolution of *Escherichia coli* lacking cellular byproduct formation for enhanced acetate utilization through compensatory ATP consumption. *Metab. Eng.*, **62**, 249–259.
63. Primak, Y.A., Du, M., Miller, M.C., Wells, D.H., Nielsen, A.T., Weyler, W. and Beck, Z.Q. (2011) Characterization of a feedback-resistant mevalonate kinase from the archaeon *Methanosarcina mazei*. *Appl. Environ. Microbiol.*, **77**, 7772–7778.
64. Luo, M.L., Mullis, A.S., Leenay, R.T. and Beisel, C.L. (2015) Repurposing endogenous type I CRISPR-Cas systems for programmable gene repression. *Nucleic Acids Res.*, **43**, 674–681.
65. Huang, H.H., Bellato, M., Qian, Y., Cárdenas, P., Pasotti, L., Magni, P. and Del Vecchio, D. (2021) dCas9 regulator to neutralize competition in CRISPRi circuits. *Nat. Commun.*, **12**, 1692.
66. Mairhofer, J., Cserjan-Puschmann, M., Striedner, G., Nöbauer, K., Razzazi-Fazeli, E. and Grabherr, R. (2010) Marker-free plasmids for gene therapeutic applications – lack of antibiotic resistance gene substantially improves the manufacturing process. *J. Biotechnol.*, **146**, 130–137.
67. Jinek, M., Chylinski, K., Fonfara, I., Hauer, M., Doudna, J.A. and Charpentier, E. (2012) A programmable dual-RNA-guided DNA endonuclease in adaptive bacterial immunity. *Science*, **337**, 816–821.
68. Zetsche, B., Gootenberg, Jonathan S., Abudayyeh, Omar O., Slaymaker, Ian M., Makarova, Kira S., Essletzbichler, P., Volz, Sara E., Joung, J., van der Oost, J., Regev, A. et al. (2015) Cpf1 is a single RNA-guided endonuclease of a class 2 CRISPR-Cas system. *Cell*, **163**, 759–771.
69. Fonfara, I., Richter, H., Bratovič, M., Le Rhun, A. and Charpentier, E. (2016) The CRISPR-associated DNA-cleaving enzyme Cpf1 also processes precursor CRISPR RNA. *Nature*, **532**, 517–521.
70. Kizer, L., Pitera, D.J., Pfleger, B.F. and Keasling, J.D. (2008) Application of functional genomics to pathway optimization for increased isoprenoid production. *Appl. Environ. Microbiol.*, **74**, 3229–3241.
71. Martin, V.J.J., Pitera, D.J., Withers, S.T., Newman, J.D. and Keasling, J.D. (2003) Engineering a mevalonate pathway in *Escherichia coli* for production of terpenoids. *Nat. Biotechnol.*, **21**, 796–802.
72. Anthony, J.R., Anthony, L.C., Nowroozi, F., Kwon, G., Newman, J.D. and Keasling, J.D. (2009) Optimization of the mevalonate-based isoprenoid biosynthetic pathway in *Escherichia coli* for production of the anti-malarial drug precursor amorpha-4,11-diene. *Metab. Eng.*, **11**, 13–19.
73. Reisch, C.R. and Prather, K.L. (2015) The no-SCAR (Scarless Cas9 Assisted Recombineering) system for genome editing in *Escherichia coli*. *Sci. Rep.*, **5**, 15096.
74. Reis, A.C., Halper, S.M., Vezeau, G.E., Cetnar, D.P., Hossain, A., Clauer, P.R. and Salis, H.M. (2019) Simultaneous repression of multiple bacterial genes using nonrepetitive extra-long sgRNA arrays. *Nat. Biotechnol.*, **37**, 1294–1301.